

Technical University of Crete  
Department of Electronic and Computer Engineering



# Equalization and pre-equalization techniques and implementation in Software Defined Radios

*Diploma Thesis*

Iliadis Stylianos

*Thesis Committee*

Professor Athanasios Liavas

Associate Professor Aggelos Bletsas

Associate Professor George N. Karystinos

Chania,  
May 2015

## Abstract

The huge expansion of wireless communication the recent decades and the increased demand for high-speed wireless connections points out the importance of efficient use of frequency bandwidth which is generally expensive and limited. Communication links between multiple transmit and receive antennas, the so-called Multiple Input and Multiple Output (MIMO) channels, have been under extensive theoretical studies for their potential to provide extra dimensions for communication, without sacrificing bandwidth resources, by multiplexing various independent data streams over the wireless medium. Optimal detection and separation of the multiplexed messages is provided by the Maximum-Likelihood method, at the cost of high complexity. The sub-optimal linear Zero-Forcing Equalization and Pre-equalization methods can drastically decrease the detection complexity at the cost of performance degradation.

Both ML and linear Equalization exploit Channel-State Information (CSI) at the receiver for retrieving the various interfering symbols. Linear pre-equalization in contrast, precancels interference at the transmitter which requires feedback in order to obtain the required CSI. The need for feedback can be avoided in Time-Division-Duplex (TDD) systems, where the transmitter can exploit the reverse-channel estimate, based on the reciprocal property of wireless propagation. Utilizing the reciprocal property in practical transceivers requires some form of calibration in order to compensate for the non-reciprocal relationship of their transmit and receive chains.

A suitable testbed for implementing and evaluating the above methods by means of Software-Defined Radio is provided by the USRP hardware platform and the GNU radio software toolkit.

# Contents

<b>1</b>	<b>Introduction</b>	<b>3</b>
1.1	Scope of the thesis . . . . .	3
1.2	Thesis outline . . . . .	4
<b>2</b>	<b>Background</b>	<b>6</b>
2.1	Digital communication . . . . .	6
2.1.1	Pulse Amplitude Modulation . . . . .	6
2.1.2	Quadrature amplitude modulation . . . . .	12
2.1.3	Detection in AWGN . . . . .	15
2.2	Wireless channels . . . . .	16
2.2.1	Time-varying and time-invariant channels . . . . .	17
2.2.2	Frequency flat and frequency selective channels . . . . .	18
2.2.3	A discrete-time flat fading model . . . . .	20
2.3	Wireless systems . . . . .	22
2.3.1	Wireless system models . . . . .	22
2.3.2	Single-user MIMO . . . . .	24
2.3.3	Multi-User MIMO . . . . .	25
2.4	Demodulation in MIMO systems . . . . .	27
2.4.1	Maximum-Likelihood detector . . . . .	27
2.4.2	Linear Zero-Forcing based detection . . . . .	28

2.4.3	Performance . . . . .	29
<b>3</b>	<b>Implementation and Results</b>	<b>32</b>
3.1	The SDR platform . . . . .	32
3.1.1	SDR basics . . . . .	32
3.1.2	USRP and GNU radio . . . . .	33
3.1.3	System configuration . . . . .	37
3.2	Processing methods . . . . .	39
3.2.1	Modulation . . . . .	39
3.2.2	Synchronization and matched-filtering . . . . .	40
3.2.3	Joint carrier-frequency-offset and channel estimation . . . . .	40
3.3	Single-user MIMO . . . . .	44
3.3.1	Maximum-Likelihood detection . . . . .	45
3.3.2	Linear Zero-Forcing Equalization . . . . .	45
3.3.3	Linear Zero-Forcing Pre-Equalization . . . . .	46
3.3.4	Performance . . . . .	49
3.4	Multi-user MIMO . . . . .	51
3.4.1	Feedback based Pre-equalization . . . . .	51
3.4.2	Exploiting the up-link CSI . . . . .	52
<b>4</b>	<b>Conclusions and future work</b>	<b>59</b>

# Chapter 1

## Introduction

### 1.1 Scope of the thesis

The huge expansion of wireless communication the recent decades and the increased demand for high-speed wireless connections points out the importance of efficient use of frequency bandwidth which is generally expensive and limited. Communication links between multiple transmit and receive antennas, the so-called Multiple Input and Multiple Output (MIMO) channels, have been under extensive theoretical studies for their potential to provide extra dimensions for communication, without sacrificing bandwidth resources. In point-to-point single-user scenarios, multiple transmit and receive antennas can be exploited for spatially-multiplexing various independent data streams on the channel, and drastically increase the rate of transmitted information. In a similar approach, the Basestation (BS) in a broadcast scenario, can use multiple transmit antennas to support various independent users simultaneously, by means of Space Division Multiple Access (SDMA).

Implementing the above techniques in practice, necessitates the study of efficient and low-complexity detection methods for retrieving the various multiplexed symbols. In this thesis, we discuss and implement the sub-optimal linear Zero-Forcing Equalization and Pre-equalization methods, and evaluate their performance with respect to the optimal but of high-complexity

Maximum-Likelihood (ML) detection rule. Both ML and linear Equalization exploit Channel-State Information (CSI) at the receiver for retrieving the various interfering messages. Linear Pre-equalization in contrast, precancels interference at the transmitter. In that case, the required CSI is usually obtained through feedback from the receiver. A calibration method that exploits the reciprocal property of the wireless medium and avoids the need for feedback is also presented in the last part of the experimental study. All the above techniques are implemented and evaluated by means of software-defined radio, using the USRP hardware platform and the GNU radio software toolkit.

## 1.2 Thesis outline

In the first chapter, we present the theoretical background of this thesis. At the beginning, we discuss some fundamental concepts of digital communication like linear modulation and detection. In the second section, we discuss the basic characteristics of the wireless medium and present the channel model that we use throughout the experimental procedure. In the third section, we give a brief overview of the various wireless system models (SISO, SIMO, MISO, and MIMO), and discuss the main characteristics of single-user and multi-user MIMO systems. In the final section of the chapter, we present the Maximum-Likelihood, linear Equalization and linear Pre-equalization detection techniques and discuss their performance.

In the second chapter, we discuss the methods and results of the experimental procedure. In the first section of the chapter, we briefly describe the design of the software-radio platform. In the second section, we discuss the basic signal processing methods we used in our implementation. In the third section, we implement, evaluate, and compare the Maximum-Likelihood and the linear Equalization and Pre-equalization techniques, through the establishment of a single-user MIMO system. In the final section of the chapter, we implement linear Pre-equalization in a multi-user scenario. At the last part of that section, we discuss and implement a calibration procedure for exploiting the reciprocal property of the wireless channel.

Finally, in the last chapter we discuss the main conclusions we drew from the experimental results and present ideas for future work.

# Chapter 2

## Background

### 2.1 Digital communication

Digital communication refers to the transmission of discrete messages over a communication channel. A fundamental concept of digital communication is modulation, that is the process of representing digital information in terms of analog waveforms, appropriate for transmission over a physical channel. Various types of modulation can be used, depending on the requirements of the communication system and the nature of the physical link. Although wireless communication typically takes place in high-frequencies (passband), the information is usually impressed and processed on equivalent baseband signals, with spectral components around the zero-frequency. In the next paragraphs, the baseband Pulse Amplitude Modulation (PAM) and the passband Quadrature Amplitude Modulation (QAM) methods are briefly discussed. Most of the context is derived by [1] and [2].

#### 2.1.1 Pulse Amplitude Modulation

Pulse amplitude modulation is a linear type of digital modulation in which information is encoded into the amplitude of baseband analog pulses. The receiver decodes the different amplitude levels of the received signal and re-produces the initial digital information.

## Mapping bits to symbols

At the first stage, the scheduled for transmission binary sequence is encoded into a sequence of real symbols that express the different voltage levels of the modulated signal. This process corresponds to the mapping

$$\{0, 1\}^K \rightarrow R^N, \quad K, N \in Z \quad (2.1)$$

and can be described as follows:

- The binary sequence is initially divided into length- $K$  groups of bits in the form  $(b_0, b_1, \dots, b_{K-1})$ .
- Each  $K$ -tuple of bits is then transformed into a  $N$ -tuple of symbols based on a mapping

$$(b_0, b_1, \dots, b_{K-1}) \mapsto (X_0, X_1, \dots, X_{N-1}) \quad (2.2)$$

which must be one-to-one so that the receiver can uniquely decode the received bit sequence.

- The so-produced  $N$ -tuples of symbols are concatenated to form the final sequence  $\{X_n\}$ .

The rate of the mapping,  $R_b = \frac{K}{N}$  is expressed in *bits per real symbol*. The set of the different possible symbols  $X_n$  that can be produced describes the constellation  $\mathcal{X}$  (or alphabet) of the modulation, and the number of elements in it is its cardinality  $|\mathcal{X}|$ .

## Pulse shaping

At the second stage, the produced symbol sequence is linearly mapped to a real and continuous-time baseband signal  $x(t)$ . For that we consider a linear low-pass filter with impulse response the pulse-shape  $g(t)$ , and input the continuous-time expression of the symbol sequence  $X_\delta(t) = \sum_n X_n \delta(t - nT)$ , where the time interval  $T$  and its reciprocal  $1/T$  are referred to as the Baud

period and the Baud rate respectively. The output is given by the convolution

$$x(t) = X_\delta(t) \star g(t) = \sum_n X_n g(t - nT), \quad t \in \mathbb{R}, \quad (2.3)$$

We assume that  $g(t)$  is a Square Root Raised Cosine (SRRC) pulse, with parameter  $T$ . These pulses have the property that their time-shifts by integer multiples of  $T$  form an orthonormal set, which means that

$$\int_{-\infty}^{\infty} g(\tau)g(\tau - kT)d\tau = \delta_k, \quad k \in Z, \quad (2.4)$$

where

$$\delta_k = \begin{cases} 1, & k = 0, \\ 0, & k \neq 0. \end{cases} \quad (2.5)$$

The importance of this property will become apparent in the process of separating the interfering waveforms, through matched-filtering at the receiver.

### The AWGN channel

Physical channels are usually band-limited and can be modeled as linear filters which generally induce attenuation and delay at the transmitted signal, and corrupt it with some form of additive noise. For simplicity we consider the ideal case of a band-limited channel without attenuation and delay, characterized by the time response  $c(t)$  and the flat frequency response  $C(f) = 1$ , for the range of frequencies of the transmitted signal. At the output we assume Additive White Gaussian Noise (AWGN)  $n(t)$ , which is an uncorrelated stochastic process with

- expected value  $E(n(t)) = 0$ ,
- and auto-correlation  $R_n(t, t + \tau) = N_0\delta(\tau)$ .

The received signal  $r(t)$  can be expressed as

$$r(t) = c(t) \star x(t) + n(t) = x(t) + n(t). \quad (2.6)$$

## Recovering symbols through matched-filtering

At the receiver, the signal  $r(t)$  passes through the filter  $\overleftarrow{g}(t)$  with response matched to the transmit pulse-shape  $g(t)$ , that is

$$\overleftarrow{g}(t) = g(-t). \quad (2.7)$$

The output is given by

$$\begin{aligned} y(t) &= r(t) \star g(-t) = x(t) \star g(-t) + \underbrace{n(t) \star g(-t)}_{w(t)} \\ &= X_\delta(t) \star \underbrace{g(t) \star g(-t)}_{v(t)} + w(t) = X_\delta(t) \star v(t) + w(t) \\ &= \sum_n X_n v(t - nT) + w(t). \end{aligned} \quad (2.8)$$

Sampling  $y(t)$  by  $\{mT\}_{m \in \mathbb{Z}}$  results in:

$$\begin{aligned} y(mT) &= y(t)|_{t=mT} = \sum_n X_n v(t - nT)|_{t=mT} + w(t)|_{t=mT} \\ &= \sum_n X_n v((m - n)T) + w(mT). \end{aligned} \quad (2.9)$$

Defining  $y_m = y(mT)$ ,  $v_m = v(mT)$  and  $w_m = w(mT)$ , we get

$$\begin{aligned} y_m &= \sum_{n=0}^{N-1} X_n v_{m-n} + w_m = \underbrace{v_0 X_m}_{s_m} + \underbrace{\sum_{n \neq m} X_n v_{m-n}}_{I_m} + w_m \\ &= v_0 X_m + I_m + w_m. \end{aligned} \quad (2.10)$$

Recalling the orthonormality of the SSRC pulse, we get that the samples of the combined

impulse response  $v(t) = g(t) \star g(-t)$  at the integer multiples  $\{kT\}$  is equal to

$$\begin{aligned} v(kT) &= v(t)|_{t=kT} = g(t) \star g(-t)|_{t=kT} \\ &= \int_{-\infty}^{\infty} g(\tau)g(\tau - kT)d\tau = \delta_k. \end{aligned} \quad (2.11)$$

Thus for the expression of the sampled output  $y_m$  in (2.10) we get that

- the term  $s_m$  which expresses the contribution of the current input symbol  $X_m$ , equals to

$$s_m = v_0 X_m = \delta_0 X_m = X_m, \quad (2.12)$$

- the term  $I_m$  which expresses the Inter-Symbol Interference (ISI) caused by the rest symbols  $X_{n \neq m}$  equals to

$$I_m = \sum_{n \neq m} X_n \underbrace{v_{m-n}}_k = \sum_{k \neq 0} X_{m-k} v_k = \sum_{k \neq 0} X_{m-k} \delta_k = 0, \quad (2.13)$$

- and the terms  $w_m$  which correspond to the sampled filtered noise, have expected value

$$E[w_m] = \int_{-\infty}^{\infty} E(n(\tau))g(\tau - mT)d\tau = 0, \quad (2.14)$$

and auto-correlation

$$\begin{aligned} R_w(m, m+k) &= E[w_m w_{m+k}] = \int_{-\infty}^{\infty} \int_{-\infty}^{\infty} \underbrace{E(n(\tau)n(\tau'))}_{N_0 \delta(\tau' - \tau)} g(\tau - mT)g(\tau' - (m+k)T)d\tau' d\tau \\ &= N_0 \int_{-\infty}^{\infty} g(\underbrace{\tau - mT}_{\tau'})g(\tau - (m+k)T)d\tau = N_0 \int_{-\infty}^{\infty} g(\tau')g(\tau' - kT)d\tau' \\ &= N_0 \delta_k. \end{aligned} \quad (2.15)$$

Consequently, the sampled output  $y_m$  takes the form

$$y_m = X_m + w_m, \quad (2.16)$$

where  $w_m$  are i.i.d. with variance  $\sigma_{w_m}^2 = N_0$ . Based on  $y_m$  the receiver recovers the initial symbol sequence through a detection process that will be discussed later on this section.

It is worth noting that the Signal to Noise Ratio (SNR) is maximized at the output of the matched filter, at the corresponding sample moments  $\{mT\}$ . In our case the maximized SNR is given by

$$SNR_{y_m} = \frac{E[X_m^2]}{E[w_m^2]} = \frac{\mathcal{E}_{X_m}}{N_0}, \quad (2.17)$$

where  $\mathcal{E}_{X_m}$  is the power of the symbols  $X_m$ .

### Bandwidth considerations

The combined response  $u(t) = g(t) \star g(-t)$ , due to the fact that it satisfies (2.11), is a so-called Nyquist pulse with parameter  $T$ , known from preventing ISI. It can be proved that satisfying (2.11) for a given  $T$  bounds the smallest possible (positive) bandwidth  $W$  of  $g(t)$ , by

$$W \geq \frac{1}{2T}. \quad (2.18)$$

Equality is met by the *sinc* pulse which therefore offers the highest spectral efficiency. Sinc-pulses are seldom used in practice, due to the fact that they decay slowly in time. The bandwidth of a SRRC pulse is given by

$$W = \frac{1 + \beta}{2T} > \frac{1}{2T}, \quad (2.19)$$

and is characterized by a controllable roll-off factor  $0 < \beta \leq 1$ , which is the ratio of the excess bandwidth of the pulse with respect to the lowest-bound  $1/2T$ .

### 2.1.2 Quadrature amplitude modulation

The signals encountered in wireless communication are usually passband. In order to transmit a baseband PAM signal over a passband channel it must be mixed (multiplied) with a periodic signal i.e.,  $\cos(2\pi f_c t)$ , named the carrier, to shift its frequency spectrum around  $f_c$ . Mixing a real baseband signal with a carrier is spectrally inefficient since it doubles its useful bandwidth. In order to compensate for this redundancy, a second independently modulated PAM signal can be mixed with a shifted by  $90^\circ$  version of the carrier and transmitted simultaneously. This is the concept of Quadrature Amplitude Modulation (QAM). We consider the PAM signals

$$\begin{aligned} x_I(t) &= \sum_n X_{I,n} g(t - nT), \\ x_Q(t) &= \sum_n X_{Q,n} g(t - nT), \end{aligned} \tag{2.20}$$

where  $X_{I,n}$ ,  $X_{Q,n}$  are independent symbol sequences each taken from the constellations  $\mathcal{X}_I$  and  $\mathcal{X}_Q$  respectively, and  $g(t)$  a SRRC pulse with parameter  $T$ . The produced two-dimensional passband signal is in the form

$$s(t) = x_I(t) \cos(2\pi f_c t) + x_Q(t) \sin(2\pi f_c t), \tag{2.21}$$

where  $x_I(t)$  and  $x_Q(t)$  are referred to as the In-phase and Quadrature components of  $s(t)$  respectively. The orthogonal relationship of the carriers allows for recovering the two message bearing signals independently and without interference from each other. In particular, the output  $r(t)$  of the ideal passband AWGN channel, is mixed in parallel with  $\cos(2\pi f_c t)$  and  $-\sin(2\pi f_c t)$  as in Figure 2.1. Utilizing simple trigonometric identities, it can be proved that

$$r(t) \cdot \cos(2\pi f_c t) = x_I(t) + n_I(t) + \Delta[2f_c], \tag{2.22}$$

and

$$r(t) \cdot (-\sin(2\pi f_c t)) = x_Q(t) + n_Q(t) + \Delta[2f_c], \quad (2.23)$$

where  $\Delta[2f_c]$  expresses signal components with frequency around  $\pm 2f_c$ , while  $n_I(t)$  and  $n_Q(t)$  are the AWGN noise signals at the output of each mixing branch, which are assumed jointly uncorrelated. The remaining high frequency terms  $\Delta[2f_c]$  are removed by the matched-filters  $\overleftarrow{g}(t)$ . The corresponding outputs of each filter namely  $y_I(t)$  and  $y_Q(t)$  are given by

$$y_I(t) = \sum_{n=0}^{N-1} X_{I,n} v(t - nT) + w_I(t), \quad (2.24)$$

and

$$y_Q(t) = \sum_{n=0}^{N-1} X_{Q,n} v(t - nT) + w_Q(t), \quad (2.25)$$

and the sampling by  $\{mT\}$  results in the noisy symbol sequences

$$y_{I,m} = X_{I,m} + w_{I,m}, \quad (2.26)$$

and

$$y_{Q,m} = X_{Q,m} + w_{Q,m}, \quad (2.27)$$

where the noise terms  $w_{I,m}$ ,  $w_{Q,m}$  are jointly i.i.d. with  $w_{I,m}, w_{Q,m} \sim N(0, N_0)$ .

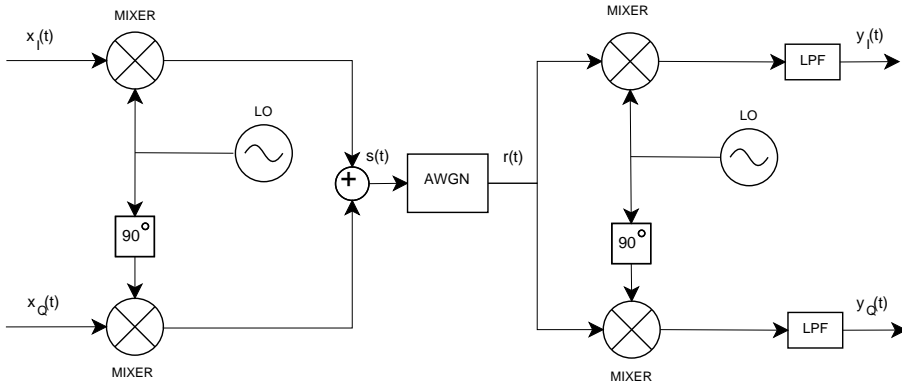


Figure 2.1: Quadrature amplitude modulation and demodulation.

## Complex baseband representation

The QAM signal in (2.21) can be equivalently expressed as

$$s(t) = \text{Re}\{x(t) \cdot e^{j2\pi f_c t}\}, \quad (2.28)$$

where  $x(t) = x_I(t) + jx_Q(t)$ , which is referred to as the baseband complex equivalent (or complex envelope) of  $s(t)$  and can be further analyzed to

$$\begin{aligned} x(t) &= \sum_n X_{I,n}g(t - nT) + j \sum_n X_{Q,n}g(t - nT) \\ &= \sum_n \underbrace{(X_{I,n} + jX_{Q,n})}_{X_n} \cdot g(t - nT) \\ &= \sum_n X_n \cdot g(t - nT). \end{aligned} \quad (2.29)$$

Similarly, the corresponding complex baseband output of the matched filter at the receiver  $y(t) = y_I(t) + jy_Q(t)$ , can be expressed as

$$y(t) = \sum_n X_n \cdot v(t - nT) + w(t), \quad (2.30)$$

with  $w(t) = w_I(t) + jw_Q(t)$ . Sampling by  $mT$  results in the complex sequence

$$y_m = X_m + w_m \quad (2.31)$$

where  $w_m \sim CN(0, 2N_0)$  are complex Gaussian noise terms. The complex symbols  $X = X_I + jX_Q$  are part of the QAM constellation  $\mathcal{X} \subset \mathbb{C}$  which is derived by the Cartesian product of the corresponding real PAM constellations  $\mathcal{X}_I$  and  $\mathcal{X}_Q$ , that is

$$\mathcal{X} := \{a + jb : (a, b) \in \mathcal{X}_I \times \mathcal{X}_Q\}, \quad (2.32)$$

and has cardinality  $|\mathcal{X}| = |\mathcal{X}|_I \cdot |\mathcal{X}|_Q$ . Geometrical representations of QAM constellations are depicted in Figure 2.2.

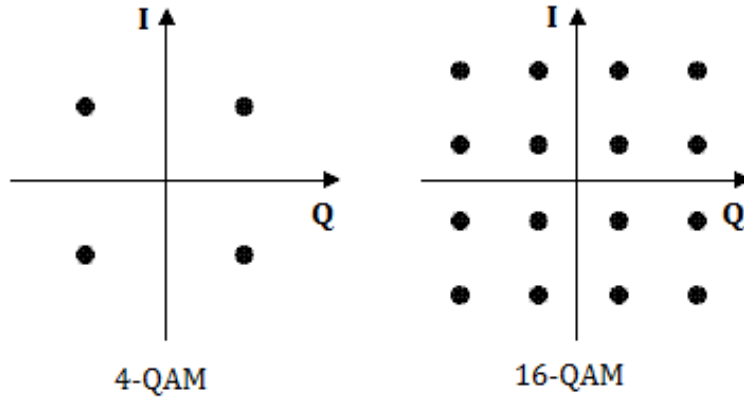


Figure 2.2: 4-QAM and 16-QAM constellations.

### 2.1.3 Detection in AWGN

The aim of detection is to recover the initial symbol sequence  $\{X_m\}$ , based on the corrupted received sequence  $\{y_m\}$ . Under the assumption that the symbols are chosen independently from each other, from the constellation  $\mathcal{X} \subset \mathbb{C} = \{x_1, x_2, \dots, x_M\}$ , optimal detection can be performed symbol by symbol based on a decision rule

$$DR : \mathbb{C} \rightarrow \{1, 2, \dots, M\}. \quad (2.33)$$

In the case of the ideal AWGN channel, the decision relies on the corresponding observation

$$Y = X + W \quad (2.34)$$

where

- $X \in \mathcal{X}$  is a discrete random variable that describes the current input, with possible outcomes the elements of the constellation  $\{x_1, x_2, \dots, x_M\}$ ,

- $W \in \mathbb{C}$  is a continuous random variable that describes the complex Gaussian noise term with  $W \sim CN(0, \sigma_w^2)$ ,
- and  $Y \in \mathbb{C}$  is a continuous random variable that describes the corresponding output with conditional probability density function (pdf) for a given  $X = x_m$  expressed by

$$f_{Y|X=x_m}(y) = \frac{1}{\sqrt{2\pi\sigma_w^2}} e^{-\frac{|y-x_m|^2}{2\sigma_w^2}}. \quad (2.35)$$

If the probability mass function  $P_X(X)$  of  $X$  is uniformly distributed over  $\mathcal{X}$ , the optimal decision in terms of minimum error probability is the Maximum Likelihood rule

$$ML(y) = \arg \max_{m=1,2,\dots,M} f_{Y|X=x_m}(y) \quad (2.36)$$

Assuming that we obtain the output  $Y = y$ , the ML rule decides for  $X = x_{\hat{m}}$  if and only if

$$\begin{aligned} f_{Y|X=x_{\hat{m}}}(y) &= \max_{m=1,2,\dots,M} f_{Y|X=x_m}(y) \\ \Leftrightarrow \frac{1}{\sqrt{2\pi\sigma_w^2}} e^{-\frac{|y-x_{\hat{m}}|^2}{2\sigma_w^2}} &= \max_{m=1,2,\dots,M} \frac{1}{\sqrt{2\pi\sigma_w^2}} e^{-\frac{|y-x_m|^2}{2\sigma_w^2}} \\ \Leftrightarrow |y - x_{\hat{m}}|^2 &= \min_{m=1,2,\dots,M} |y - x_m|^2. \end{aligned} \quad (2.37)$$

thus it results in the rule of the nearest neighbor.

## 2.2 Wireless channels

Unlike wired channels, whose characteristics are usually stationary and predictable, the performance of wireless transmissions is highly dependent on the constantly varying conditions of the outdoor environment. Good characterization and modeling of the wireless channel is therefore crucial to the design of reliable wireless systems. The various phenomena related with wireless propagation can be roughly divided into two types:

- Large-scale phenomena associated with the attenuation of the signal due to the distance between the transmitter and the receiver or due to shadowing by large objects such as buildings and hills. Those phenomena usually vary slowly in time and mainly depend on the topology of the wireless system.
- Small-scale phenomena that concern the fast variations of the channel in time and frequency due to mobility of the transmitter, the receiver and the obstacles between them, and due to the multipath propagation of the signals in the wireless medium.

Multipath propagation is caused by the reflection, defraction and scattering of the signal, due to the various objects in the environment, which create multiple signal paths each with different delay and attenuation. As a result, the received signal contains either constructive or destructive superposition of multiple delayed and attenuated copies of the transmitted signal. Multipath wireless channels can be well-modeled as linear time-varying filters with impulse response

$$c(\tau, t) = \sum_{l=1}^{L(t)} \alpha_l(t) \delta(t - \tau_l(t)), \quad (2.38)$$

where  $L(t)$  is the number of the separable paths, and  $\alpha_l(t)$  is the corresponding gain of each path.

The properties of the wireless medium together with the nature of the signal characterize the channel in time and frequency. Different channel models, in terms of time and frequency selectivity, are briefly discussed in the following paragraphs. The context of this section is mostly derived by [3].

### 2.2.1 Time-varying and time-invariant channels

A baseband equivalent model for the response of the physical channel in (2.38) can be expressed as

$$h(\tau, t) = \sum_{l=1}^{L(t)} \alpha_l(t) \delta(t - \tau_l(t)). \quad (2.39)$$

where now the gains  $\alpha_l(t)$  are complex numbers each with different amplitude and phase. The various gains and delays as well as the number of the paths are time dependent. Supposing that  $x(t)$  and  $y(t)$  are the baseband input and output signals of such a channel, their relationship is given by

$$y(t) = h(\tau, t) * x(t) + n(t) = \sum_{l=1}^{L(t)} \alpha_l(t) x(t - \tau_l(t)) + n(t) \quad (2.40)$$

where  $n(t)$  is the additive noise.

Assuming that the environment, as well as the transmitter and the receiver are stationary, the channel can be described as a time-invariant filter with response

$$h(\tau) = \sum_{l=1}^L \alpha_l \delta(t - \tau_l), \quad (2.41)$$

and the input-output relationship takes the form

$$y(t) = h(\tau, t) * x(t) + n(t) = \sum_{l=1}^L \alpha_l x(t - \tau_l) + n(t). \quad (2.42)$$

Time-invariant channel models greatly simplify the processing of the output signal, but are unrealistic in practice. A more realistic approach assumes the channel approximately constant only for the duration of the transmission of an information block. This type of channel model is referred to as block-fading.

### 2.2.2 Frequency flat and frequency selective channels

An important characteristic of multipath propagation is the so-called delay-spread parameter  $T_d$ , which is the time difference between the longest and the shortest propagation path. For time-invariant channels the delay-spread can be expressed as

$$T_d = \max_{i,j} |\tau_i - \tau_j|. \quad (2.43)$$

Reciprocal to the delay spread is the coherence bandwidth

$$B_c \approx \frac{1}{T_d}, \quad (2.44)$$

which expresses the frequency range at which the channel response is highly correlated and thus can be considered flat.

### Frequency selective channels

If the delay spread is comparable or greater than the baud period  $T$ , that is

$$T_d \gtrsim T, \quad (2.45)$$

or equivalently if the coherence bandwidth is comparable or less than the bandwidth  $W$  of the signal, that is

$$B_c \lesssim W, \quad (2.46)$$

then each received symbol is usually distorted by the delayed arrival of previously transmitted symbols, and therefore the output of the channel suffers from *ISI*. This type of fading is referred to as frequency selective, and derives its name by the fact that it results in non-uniform attenuation of the frequency components of the received signal.

### Frequency flat channels

On the contrary, if the delay-spread is significantly less than  $T$ , that is

$$T_d \ll T, \quad (2.47)$$

or equivalently if

$$B_c \gg W, \quad (2.48)$$

the different delays of the channel paths can be assumed approximately equal, that is

$$\tau_l \approx \bar{\tau}, \quad l = 1, \dots, L. \quad (2.49)$$

In that case the channel response can be expressed as

$$c(\tau) \approx \underbrace{\sum_{l=1}^L \alpha_l}_{c} \delta(t - \bar{\tau}) = c \cdot \delta(t - \bar{\tau}). \quad (2.50)$$

meaning that the different delayed paths can be reduced to one dominant path with delay  $\bar{\tau}$  and therefore ISI is prevented. This type of fading is referred to as flat since it results in uniform attenuation of the frequency components of the received signal.

### 2.2.3 A discrete-time flat fading model

We consider the baseband signal

$$x(t) = \sum_n X_n g(t - nT) \quad (2.51)$$

where  $g(t)$  is a SRRC pulse and  $X_n$  a complex symbol sequence. We assume a time-invariant flat-fading baseband channel with response  $c(\tau) = c \cdot \delta(t - \bar{\tau})$  where  $c \in \mathbb{C}$  and complex AWGN noise  $n(t)$  at the output. The received signal passes through the matched filter  $\overleftarrow{g}(t) = g(-t)$ ,

the output of which is given by

$$\begin{aligned}
y(t) &= (x(t) \star c(t) \star n(t)) \star g(-t) \\
&= x(t) \star c(t) \star g(-t) + \underbrace{n(t) \star g(-t)}_{w(t)} \\
&= x_\delta(t) \star \underbrace{g(t) \star c(t) \star g(-t)}_{h(t)} + w(t) \\
&= \sum_n X_n h(t - nT) + w(t)
\end{aligned} \tag{2.52}$$

where

$$h(t) = g(t) \star c(t) \star g(-t) = c(t) \star \underbrace{g(t) \star g(-t)}_{v(t)} = c \cdot \delta(t - \bar{\tau}) \star v(t) = cv(t - \bar{\tau}). \tag{2.53}$$

Therefore  $y(t)$  can be expressed as

$$y(t) = \sum_n X_n v(t - nT - \bar{\tau}). \tag{2.54}$$

Sampling at  $t = mT + \bar{\tau}$  and recalling that  $v(t)$  is a Nyquist pulse we get

$$\begin{aligned}
y_m &= y(t)|_{t=mT+\bar{\tau}} \\
&= \sum_n X_n c \cdot v(t - nT - \bar{\tau}) + w(t)|_{t=mT+\bar{\tau}} \\
&= c \cdot \sum_n X_n v(mT - nT) + \underbrace{w(mT + \bar{\tau})}_{w_m} \\
&= cX_m + w_m,
\end{aligned} \tag{2.55}$$

with  $w \sim \mathcal{CN}(0, \sigma_w^2)$ . Therefore the channel induces a complex gain  $c$  without ISI. This is the channel model that we will consider for the rest of this thesis.

## 2.3 Wireless systems

### 2.3.1 Wireless system models

#### Single-input/single-output system

A single-input/single-output (SISO) system model, can be described by

$$y = hx + w, \quad (2.56)$$

where

- $x, y \in \mathbb{C}$  are the discrete input and discrete output respectively,
- $h \in \mathbb{C}$  is the channel coefficient and
- $w \sim \mathcal{CN}(0, \sigma_w^2)$  is the complex Gaussian noise term.

#### Multiple-input/single-output system

A multiple-input/single-output (MISO) system model, with  $N_T > 1$  transmit and one receive antenna, can be expressed as

$$y = h_1x_1 + h_2x_2 + \dots + h_{N_T}x_{N_T} + w \quad (2.57)$$

or equivalently in vector form

$$y = \mathbf{h}^T \mathbf{x} + w \quad (2.58)$$

where  $\mathbf{h} = [h_1, h_2, \dots, h_{N_T}]^T$  is the channel vector and  $\mathbf{x} = [x_1, x_2, \dots, x_{N_T}]^T$  the input vector.

### Single-input/multiple-output system

A single-input/multiple-output (SIMO) system model, with one transmit and  $N_R > 1$  receive antennas can be expressed by the system of equations

$$\begin{aligned}y_1 &= h_1x + w_1 \\y_2 &= h_2x + w_2 \\&\vdots \\y_{N_R} &= h_{N_R}x + w_{N_R},\end{aligned}\tag{2.59}$$

or equivalently in vector form

$$\mathbf{y} = \mathbf{h}x + \mathbf{w}\tag{2.60}$$

where

- $\mathbf{y} = [y_1, y_2, \dots, y_{N_R}]^T$  is the output vector,
- $\mathbf{h} = [h_1, h_2, \dots, h_{N_R}]^T$  the channel vector and
- $\mathbf{w} = [w_1, w_2, \dots, w_{N_R}]^T$  the noise vector with  $\mathbf{w} \sim \mathcal{CN}(0, \sigma_w^2 \cdot \mathbf{I})$ .

### Multiple-input/multiple-output system

A multiple-input/multiple-output (MIMO) system model, with  $N_T, N_R > 1$  transmit and receive antennas, respectively, can be expressed by the system of equations

$$\begin{aligned}y_1 &= h_{1,1}x_1 + h_{1,2}x_2 + \dots + h_{1,N_T}x_{N_T} + w_1 \\y_2 &= h_{2,1}x_1 + h_{2,2}x_2 + \dots + h_{2,N_T}x_{N_T} + w_2 \\&\vdots \\y_{N_R} &= h_{N_R,1}x_1 + h_{N_R,2}x_2 + \dots + h_{N_R,N_T}x_{N_T} + w_{N_R},\end{aligned}\tag{2.61}$$

or equivalently in matrix form

$$\mathbf{y} = \mathbf{H}\mathbf{x} + \mathbf{w}, \quad (2.62)$$

where

- $\mathbf{y} = [y_1, y_2, \dots, y_{N_R}]^T$  is the output vector,
- $\mathbf{x} = [x_1, x_2, \dots, x_{N_T}]^T$  the input vector,
- $\mathbf{H} = \begin{bmatrix} h_{1,1} & h_{1,2} & \dots & h_{1,N_T} \\ h_{2,1} & h_{2,2} & \dots & h_{2,N_T} \\ \vdots & \vdots & \ddots & \vdots \\ h_{N_R,1} & h_{N_R,2} & \dots & h_{N_R,N_T} \end{bmatrix}$  is the channel matrix and
- $\mathbf{w} = [w_1, w_2, \dots, w_{N_R}]^T$  the noise vector with  $\mathbf{w} \sim \mathcal{CN}(0, \sigma_w^2 \cdot \mathbf{I})$ .

### 2.3.2 Single-user MIMO

Single-user MIMO refers to a point to point MIMO case, where both sides have multiple co-located antennas, which can be utilized to jointly process the parallel transmitted and received data streams (Fig. 2.3).

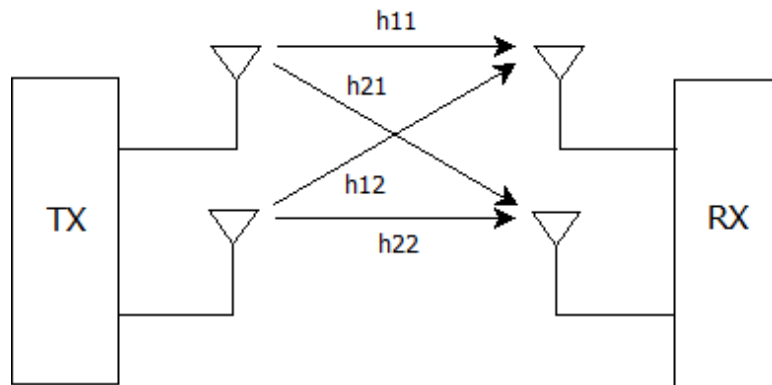


Figure 2.3: Single-user MIMO.

## Spatial multiplexing

The multiple transmit and receive antennas in a single-user MIMO system, can add extra degrees of freedom for communication. Considering a full-rank  $N_T \times N_R$  channel matrix  $\mathbf{H}$ , it can be proved through Singular Value Decomposition (SVD) [4], that the matrix can be converted into a set of  $k = \min(N_T, N_R)$  parallel and independent sub-channels, each capable of conveying data. Therefore up to  $k$  independent data-streams can be multiplexed and reliably transmitted through the full-rank MIMO channel, increasing in that sense data-rates without the need for bandwidth expansion. This is referred to as *spatial multiplexing*. In point-to-point systems, the use of co-located antennas may increase the spatial correlation of the multiple paths, and consequently result in loss of rank of the channel matrix. In order to achieve the full spatial multiplexing capability of the MIMO channel in that case, the scattering environment must be sufficiently rich so that the rows and columns of  $\mathbf{H}$  remain linearly independent. This is an example where multipath propagation can be proved beneficial to communication.

### 2.3.3 Multi-User MIMO

A typical multi-user MIMO scenario consists of an access point with multiple antennas, usually referred to as the Base-Station (BS), and various independent users with one antenna each. In that case only the antennas of the BS can cooperate to jointly process all the parallel data streams. Multi-User MIMO channels are distinguished between the forward (or down-link) and the reverse (or up-link) channel. The forward-link (from the BS to the independent users), is a point to multi-point MIMO Broadcast-Channel (BC) (Fig 2.4 ), while the reverse-link (from the independent users to the BS), is a multi-point to point, MIMO Multiple-Access-Channel (MAC).

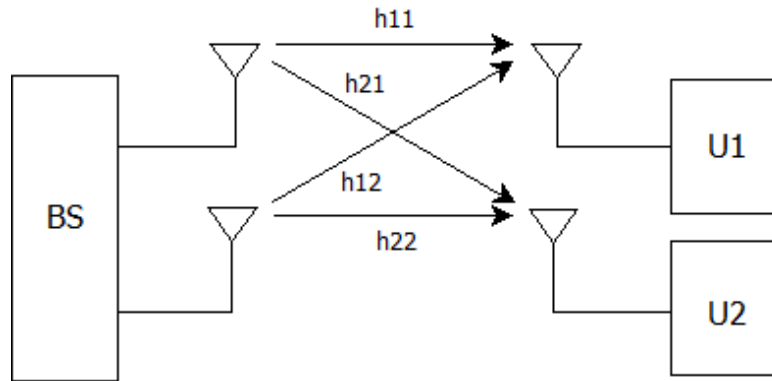


Figure 2.4: MIMO-BC.

### Space-Division Multiple Access for downlink

We consider the downlink transmission in a multi-user MIMO system with  $N_T$  transmit antennas at the BS, and  $N_R$  receive antennas each placed at a single independent user. The spatial separation of the users can be exploited by simultaneously allocating the available bandwidth to up to  $k = \min(N_T, N_R)$  independent users. This is a type of Space Division Multiple Access (SDMA). Although the total channel can support up to  $k$  independent users, the individual paths between the  $N_T$  antennas of the BS and each user correspond to a MISO channel, with maximum multiplexing capability limited to  $\min(N_T, 1) = 1$ . In other words, each single-antenna user does not have the available degrees of freedom to separate multiple interfering data-streams. Thus, achieving the maximum capability of the MIMO channel, requires some form of precoding at the transmit antennas of the BS, in order to mitigate the resulting co-channel interference.

### Channel state information at the transmitter

Pre-canceling interference at the transmitter essentially requires short-term knowledge of the downlink channel matrix. This Channel State Information (CSI) is usually obtained by employing a feedback link through which the downlink channel estimates of each user are fed back to the BS. In a fast varying spatial environment, CSI should be updated regularly, pushing a significant overhead on the system and binding resources that would be otherwise used for data

transmission. The feedback overhead can be avoided in Time-Division-Duplex (TDD) systems, where the uplink and downlink transmissions take place on the same frequency band. In that case, the BS can utilize the uplink estimate to obtain the required downlink CSI, based on the principle of reciprocity of wireless propagation, which states that the radiation pattern between two antennas is the same at both directions. In practice, although the wireless medium is reciprocal, the transmit and receive chains of the transceivers are not in general, which necessitates some form of calibration to practically utilize the reciprocal property of the physical channel.

## 2.4 Demodulation in MIMO systems

The context of this section is derived by [5] and [6].

### 2.4.1 Maximum-Likelihood detector

We consider a frequency-flat and time-invariant MIMO channel, with  $N_T$  transmit and  $N_R$  receive antennas, described by

$$\mathbf{y} = \mathbf{H}\mathbf{x} + \mathbf{w} \quad (2.63)$$

where the elements of the transmitted vector  $\mathbf{x}$  are chosen independently from a constellation  $\mathcal{X}$  and  $\mathbf{w}_N \sim \mathcal{CN}(0, \sigma_w^2 \cdot \mathbf{I})$  is AWGN vector. The aim of the receiver is to obtain an estimate of  $\mathbf{x}$ , based on  $\mathbf{y}$  and an estimate of the channel matrix  $\mathbf{H}$ . Maximum-Likelihood (ML) detection provides the optimal estimation of  $\mathbf{x}$ , in the sense of minimum error probability. The detection results in the message  $\hat{\mathbf{x}}$  which yields the smallest distance between the received vector  $\mathbf{y}$  and the hypothesized message  $\mathbf{H}\hat{\mathbf{x}}$ , through exhaustive search over the set  $\mathcal{X}^{N_T}$ . The ML estimate  $\hat{\mathbf{x}}_{ML}$  is given by

$$\hat{\mathbf{x}}_{ML} = \arg \min_{\mathbf{x} \in \mathcal{X}^{N_T}} \left( \|\mathbf{y} - \mathbf{H}\hat{\mathbf{x}}\| \right). \quad (2.64)$$

The optimality of ML-detection comes at the cost of high complexity. The cardinality of the set of the possible transmitted vectors is  $|\mathcal{X}|^{N_T}$  and therefore the number of the required search steps increases exponentially with the number of transmit antennas  $N_T$ . As a result, the complexity can grow prohibitively large for high order MIMO systems.

### 2.4.2 Linear Zero-Forcing based detection

The complexity of detection can be effectively reduced by removing the interference caused by the multiple transmitted data streams. In case where the channel paths fade independently, each symbol reaches the receiver with a distinct spatial signature and can be conveniently separated through linear transformations that result in cancellation of the interfering symbols. This forms a sub-optimal method referred to as Linear Zero-Forcing (ZF) based detection. In the case of  $N_T$  transmit and  $N_R$  receive antennas and full-rank channel matrix  $\mathbf{H}$ , up to  $k = \min[N_T, N_R]$  independent symbols can be extracted. The separation is performed through a ZF-matrix  $\mathbf{G}_{ZF}$ , which resolves  $\mathbf{H}$  into  $K$  non-interfering, point to point sub-channels. Under certain conditions, the ZF-matrix can be applied either at the received vector, forming a ZF Equalization scheme, or pre-applied at the transmitted vector resulting in a ZF Pre-Equalization scheme respectively.

#### Zero-Forcing Equalization

For the general  $N_T \times N_R$  case, with  $N_R \geq N_T$ , linear ZF-Equalization over the channel matrix  $\mathbf{H}$ , is performed by applying at the received vector a  $(N_T \times N_R)$  matrix  $\mathbf{G}_{ZF}$  such that

$$\mathbf{G}_{ZF} \cdot \mathbf{H} = \mathbf{I}. \quad (2.65)$$

For square ( $N \times N$ ) channel matrix  $\mathbf{H}$ ,  $\mathbf{G}_{ZF}$  is given by the inverse  $\mathbf{H}^{-1}$ . In that case, assuming perfect channel knowledge, Zero-Forcing Equalization is described by

$$\mathbf{y}_{ZF} = \mathbf{H}^{-1} \cdot \mathbf{y} = \mathbf{H}^{-1} \mathbf{H} \cdot \mathbf{x} + \mathbf{H}^{-1} \cdot \mathbf{w} = \mathbf{x} + \bar{\mathbf{w}} \quad (2.66)$$

where  $\bar{\mathbf{w}} = \mathbf{H}^{-1}\mathbf{w}$ . By separating the interfering streams, the decision over the transmitted symbols can be taken individually, similarly to the point to point case. The minimization criterion for each estimate  $\hat{x}_i$  for  $i = 1, \dots, N_T$ , is given by

$$\hat{x}_{iZF} = \arg \min_{\hat{x} \in \mathcal{X}} \left( \|y_{iZF} - \hat{x}\| \right) \quad (2.67)$$

and the number of the total required search steps for estimating the  $N_T$  symbols is  $|\mathcal{X}| \cdot N_T$ , which grows linearly with number of transmit antennas. Thus Zero-Forcing provides a low complexity detection method for high order MIMO systems.

### Zero-Forcing Pre-Equalization

For the  $N_T \times N_R$  case, with  $N_T \leq N_R$ , given that the channel matrix is known at the transmitter, ZF Pre-Equalization is performed by transforming the transmitted vector with a  $(N_T \times N_R)$  matrix  $\mathbf{G}_{ZF}$  such that

$$\mathbf{H} \cdot \mathbf{G}_{ZF} = \mathbf{I}. \quad (2.68)$$

For square  $H$ , the transformed transmitted vector is given by  $\mathbf{x}_{ZF} = \mathbf{H}^{-1} \cdot \mathbf{x}$ . Assuming perfect channel knowledge, ZF Pre-Equalization results in

$$y_{ZF} = \mathbf{H} \cdot \mathbf{x}_{ZF} + \mathbf{w} = \mathbf{x} + \mathbf{w}. \quad (2.69)$$

Pre-Equalization is particularly suitable for communication systems with more processing power available at the transmitter or multi-user MIMO scenarios where only the Basestation can be fully aware of the channel matrix  $\mathbf{H}$ .

### 2.4.3 Performance

Zero-Forcing Equalization and Pre-Equalization are sub-optimal methods that are known to suffer from poor power efficiency especially in the cases of ill-conditioned channel matrices. In

the equalization scheme described by (2.66), the transformed noise  $\bar{\mathbf{w}} = \mathbf{H}^{-1}\mathbf{w}$  is enhanced by the effect of the equalization matrix  $\mathbf{H}^{-1}$ . This noise enhancement degrades the SNR and consequently the throughput of the channel. Assuming i.i.d. symbols, the covariance matrix of  $\mathbf{x}$  is given by  $\text{cov}(\mathbf{x}) = \sigma_x^2 \cdot \mathbf{I}_N$ , where  $\sigma_x^2$  is the mean power of the transmitted symbols. Then, we can denote the received SNR before equalization as:

$$SNR_{ML} = \frac{\text{tr}(\mathbf{H}\text{cov}(\mathbf{x})\mathbf{H}^H)}{\text{tr}(\text{cov}(\mathbf{w}))} = \frac{\sigma_x^2 \text{tr}(\mathbf{H}\mathbf{H}^H)}{\sigma_w^2 N}, \quad (2.70)$$

where  $\text{tr}(\cdot)$  denotes the matrix trace. After zero-forcing equalization, the SNR is given by:

$$SNR_{EQ} = \frac{\text{tr}(\text{cov}(\mathbf{x}))}{\text{tr}(\text{cov}(\bar{\mathbf{w}}))} = \frac{\sigma_x^2 N}{\sigma_w^2 \text{tr}(\mathbf{H}^{-1}\mathbf{H}^{-H})}. \quad (2.71)$$

By (2.70) and (2.71) we get that  $SNR_{EQ}$  and  $SNR_{ML}$  are related as:

$$SNR_{EQ} = \frac{N^2}{\text{tr}(\mathbf{H}^{-1}\mathbf{H}^{-H})\text{tr}(\mathbf{H}\mathbf{H}^H)} SNR_{ML}. \quad (2.72)$$

For any pair of matrices  $\mathbf{A}$  and  $\mathbf{B}$  of compatible dimensions, the following property holds [7]:

$$\|\text{tr}(\mathbf{A}^H \mathbf{B})\|^2 \leq \text{tr}(\mathbf{A}^H \mathbf{A}) \cdot \text{tr}(\mathbf{B}^H \mathbf{B}). \quad (2.73)$$

Thus,

$$\text{tr}(\mathbf{H}^{-1}\mathbf{H}^{-H})\text{tr}(\mathbf{H}\mathbf{H}^H) = \text{tr}(\mathbf{H}^{-1}\mathbf{H}^{-H})\text{tr}(\mathbf{H}^H\mathbf{H}) \geq \|\text{tr}(\mathbf{H}^{-1}\mathbf{H})\|^2 = \|\text{tr}(\mathbf{I})\|^2 = N^2, \quad (2.74)$$

and therefore

$$SNR_{EQ} \leq SNR_{ML}. \quad (2.75)$$

The relationship (2.72) can be re-written as

$$SNR_{EQ} = \frac{N^2}{\|\mathbf{H}^{-1}\|_F^2 \|\mathbf{H}\|_F^2} SNR_{ML}, \quad (2.76)$$

where the term  $(\|\mathbf{H}^{-1}\|_F \|\mathbf{H}\|_F)$ , is equal to the Frobenius condition number of  $\mathbf{H}$ , which shows the degradation of SNR, when equalization is performed over channel matrices with large condition numbers. Similarly, in the Pre-Equalization case, the transmit power is boosted by the effect of  $\mathbf{H}^{-1}$  on the transmitted symbols. In order to keep the total transmit power equal to  $N\sigma_x^2$ , the Pre-Equalization matrix must be weighted by  $\beta = \frac{\sqrt{N}}{\|\mathbf{H}^{-1}\|_F}$ . In that case, the transformed transmitted vector is given by  $\mathbf{x}_{ZF} = \beta \mathbf{H}^{-1} \mathbf{x}$ , and the receiver reads

$$y_{ZF} = \mathbf{H} \cdot \mathbf{x}_{ZF} + \mathbf{w} = \beta \mathbf{x} + \mathbf{w}, \quad (2.77)$$

with SNR:

$$SNR_{PREQ} = \frac{\text{tr}(\text{cov}(\beta \mathbf{x}))}{\text{tr}(\text{cov}(\mathbf{w}))} = \frac{N\beta^2\sigma_x^2}{N\sigma_w^2} = \frac{N\sigma_x^2}{\|\mathbf{H}^{-1}\|_F^2 \sigma_w^2}, \quad (2.78)$$

which is equal to that of the Equalization case in (2.71).

# Chapter 3

## Implementation and Results

### 3.1 The SDR platform

#### 3.1.1 SDR basics

Software-Defined Radios (SDRs) provide a flexible environment for prototyping and experimenting with communication techniques. In conventional systems, most of the processing stages within modulation and demodulation of the transmitted data, that constitute the so-called *physical-layer* of a wireless protocol, are implemented in dedicated hardware and operate under fixed parameters such as a carrier frequency, a certain bandwidth and a modulation scheme. Changing these parameters requires hardware modifications, which are often time-consuming and expensive. In contrast, SDRs implement some or all of their *physical – layer* functionality by means of software, on personal computers or embedded computing devices [8]. As a result, SDRs can change some of their key radio parameters through software and flexibly interact with a variety of radio systems.

#### Currently realizable SDRs

In ideal software radios, signals are digitized at the antenna and processed completely in software. Such radios are currently unrealizable due to hardware limitations. The Nyquist's sam-

pling theorem for example, states that a signal must be sampled at a rate greater than two times its highest frequency component to avoid aliasing. Limitations in the sampling rate of current analog-to-digital converters (ADCs), and the current processing power of general-purpose processors, necessitate the use of analog Radio-Frequency (RF) front-ends, for translating signals between high RF and some low intermediate or baseband frequency, suitable for digitizing.

A typical SDR architecture is depicted in Figure 3.1. The RF-front-end typically operates in a specific RF-band and besides frequency translation provides amplification and filtering for enhancing the quality of the analog signal. A Field Programmable Gate Array (FPGA) is employed to reduce some of the computational burden of the processor. It performs general-purpose and computationally expensive digital signal processing, usually including digital up and down conversion and data interpolation and decimation.

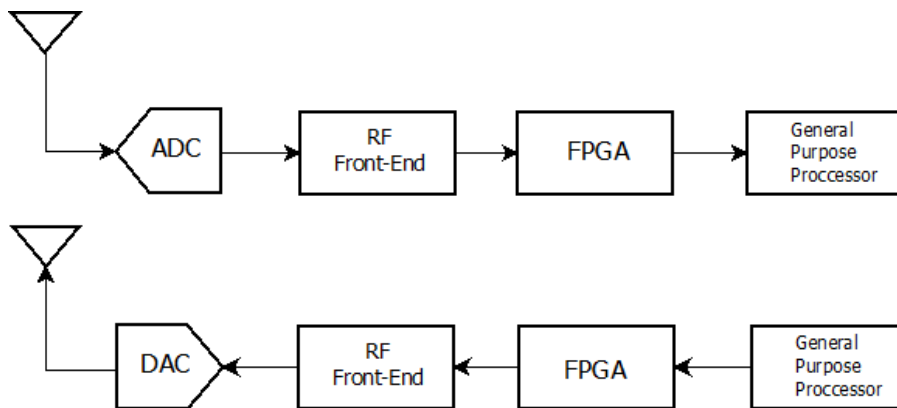


Figure 3.1: Typical SDR architecture.

### 3.1.2 USRP and GNU radio

A commonly used SDR platform within research community is the combination of the Universal Software Radio Peripheral (USRP) as a digital front-end and the GNU-Radio software as a baseband processing environment. The USRPs are a series of low-cost hardware platforms for implementing SDRs, designed and sold by Ettus Research and its parent company National

Instruments. A number of swappable RF front-ends, called *daughter-boards*, can be used in conjunction with the USRP motherboard to support frequency coverage of up to 6 GHz. All USRPs are controlled with the open-source USRP Hardware Driver (UHD), which is supported by several frameworks, including GNU Radio. Alternatively, the user can access its functionality directly through the UHD Application Programming Interface (API), which provides native support for C++.

GNU Radio is a free and open-source software development toolkit for implementing software radios. It can be used in conjunction with external hardware like USRP, or as a stand-alone simulation and development environment. The framework provides a variety of signal processing blocks like filters, equalizers and other elements that are typically found in radio systems. More importantly, it provides a method for synchronizing and connecting these blocks together, to create complicated, real-time processing applications.

For our experimental procedure, we used the USRP1 motherboard in conjunction with the RFX-2400 daughterboard as hardware platform, and the GNU Radio Companion (a graphical user-interface provided by GNU Radio) for interacting with the device. A brief description of the above tools, derived mainly by [9] and [10], is provided in the following paragraphs.

### **The RFX-2400 daughterboard**

The RFX-2400 daughterboard is complete RF transceiver system designed specifically for operation in the 2.4 GHz band. It performs quadrature mixing and direct-conversion from RF to baseband and vice versa. It has a TX/RX antenna port with a built-in transmit/receive switching that allows a single antenna to be used for transmission and reception in half-duplex mode, and an auxiliary RX2 antenna port for reception only (Figure 3.2). The LOs at the transmit and receive chain are driven by external clocking reference, enabling frequency tuning across multiple RFX-daughterboards for MIMO applications.



Figure 3.2: The RFX-2400 daughterboard.

### The USRP1 motherboard

The USRP1 is the original of the USRPs series of products. It is used in conjunction with a host PC to provide entry-level RF processing capabilities. It has four extension sockets (2 TX, 2 RX) for supporting up to two quadrature transceiver daughterboards for MIMO applications. A block-diagram of the motherboard is depicted in Figure 3.3. It includes:

- Four high-speed ADCs, each capable of 64 MS/s at a resolution of 12-bit.
- Four high-speed DACs, each capable of 128 MS/s at a resolution of 14-bit.
- An Altera Cyclone EP1C12 FPGA, the standard image of which includes:
  - Two parallel Digital Down Conversion (DDC) and decimation receive chains.
  - Two parallel Digital Up Conversion (DUC) and interpolation transmit chains.
- A Cypress EZ-USB FX2 High-speed USB 2.0 controller for streaming samples to and from the host PC.

The FPGA performs frequency translations between low IF and baseband, as well as data interpolation and decimation to reduce data-rates to something that can be transferred over USB2. The user specifies an overall center frequency for the signal chain. The RF front-end will

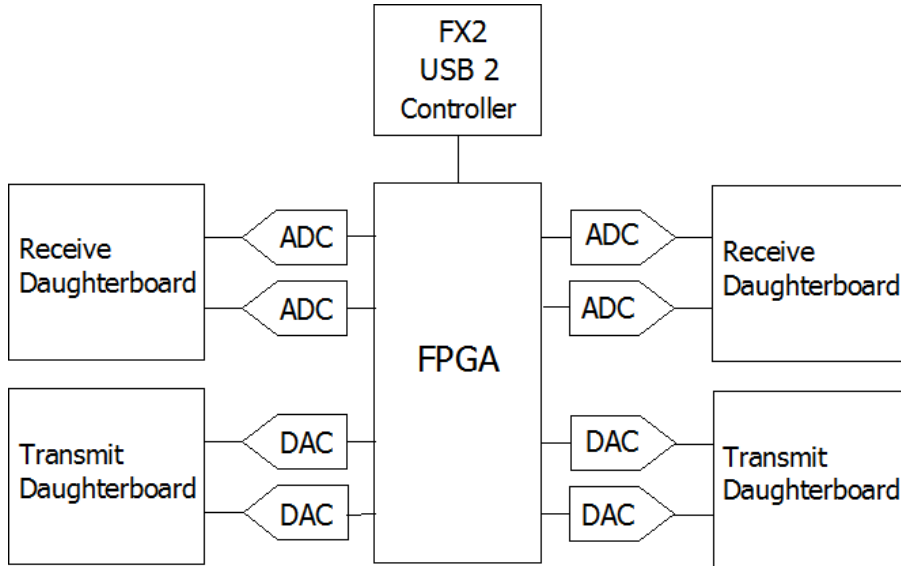


Figure 3.3: USRP1 block diagram.

be tuned as close as possible to the center frequency and the DUC and DDC chains will account for the error in tuning between target frequency and actual frequency. The decimation and interpolation factors are defined by the user and determine the available processing bandwidth on the host pc. More specifically, the host transmit sample-rate is

$$\frac{\text{DAC rate}}{\text{interpolation}} = \frac{128}{\text{interpolation}} \text{MS/sec}$$

and the host receive sample-rate is

$$\frac{\text{ADC rate}}{\text{decimation}} = \frac{64}{\text{decimation}} \text{MS/sec}$$

At transmission, interleaved baseband data that corresponds to the I and Q samples of each transmit channel is sent from the host PC and pushed into the transmit FIFO on the USRP. This data is de-interleaved and accordingly fed to the parallel DUC chains where it is interpolated and translated to IF. The output of each DUC chain is then passed to the DAC section and subsequently to the corresponding daughterboard transmit chain. At reception, the

digitized output signals of the ADC section are fed to the parallel DDC chains where they are initially down-converted and thereafter decimated. The outputs of the parallel DDC chains are interleaved and pushed into the receive FIFO of the USRP, and from there to the host PC.

## **The GNU Radio Companion**

GNU Radio applications are primarily written in Python. The various processing blocks are implemented in C++ for maximizing performance, and are exported as Python extension modules so that they can be accessed directly through Python. Instead of writing code, the user can create graphical flow-graphs to connect the various blocks together, through the GNU Radio Companion (GRC) graphical interface. During “compilation” of the flow-graph, python source code is automatically generated to execute its functionality.

### **3.1.3 System configuration**

#### **Overview**

In our test-bed we use both single-antenna and 2-antenna radio transceivers, each operating in half-duplex mode. The single-antenna transceiver consists of a USRP 1 motherboard and one RFX-2400 daughterboard. We place a single antenna on the TX/RX port for transmission and reception. Unless there is data available in the transmit FIFO of the USRP, the transceiver is always in receive mode and continuously streams received samples to the host PC.

For the 2-antenna transceiver we use two RFX-2400 daughterboards on board, each with one antenna placed on the TX/RX port. Both daughterboards are configured to use the common 64 MHz clocking reference of the motherboard, providing fine tuning and phase-locking across the two RF chains.

A host PC equipped with Linux/Ubuntu operating system and the GNU radio framework is connected through a USB cable with each USRP. We perform all the signal processing in Matlab scripts. In parallel with the running Matlab script, we execute a GNU radio flow-graph to configure the USRP parameters and stream data to and from the device. Communication

between those two parallel processes is provided by two pipe files (fifos), one for the transmit and one for the receive data stream.

### GNU Radio flow-graphs

For the single-antenna case depicted in Figure (3.4), we use one USRP-source and one USRP-sink block to stream data from and to the device, and control the associated parameters. We define equal center-frequency and gain for the transmit and receive chain. The interpolation factor is set always two times the value of decimation, so that the host transmit and receive sample rates are equal. The file-source and file-sink blocks provide interface for accessing the pipes that connect the flow-graph with the Matlab script.

For the two-antenna transceiver depicted in (3.5) we use the dual-USRP source and sink blocks. An interleave block is placed between the dual-USRP source and the file-sink block, to interleave the two receive data streams in one, before push them in the receive fifo. A deinterleaver performs the opposite operation for the transmit chain.

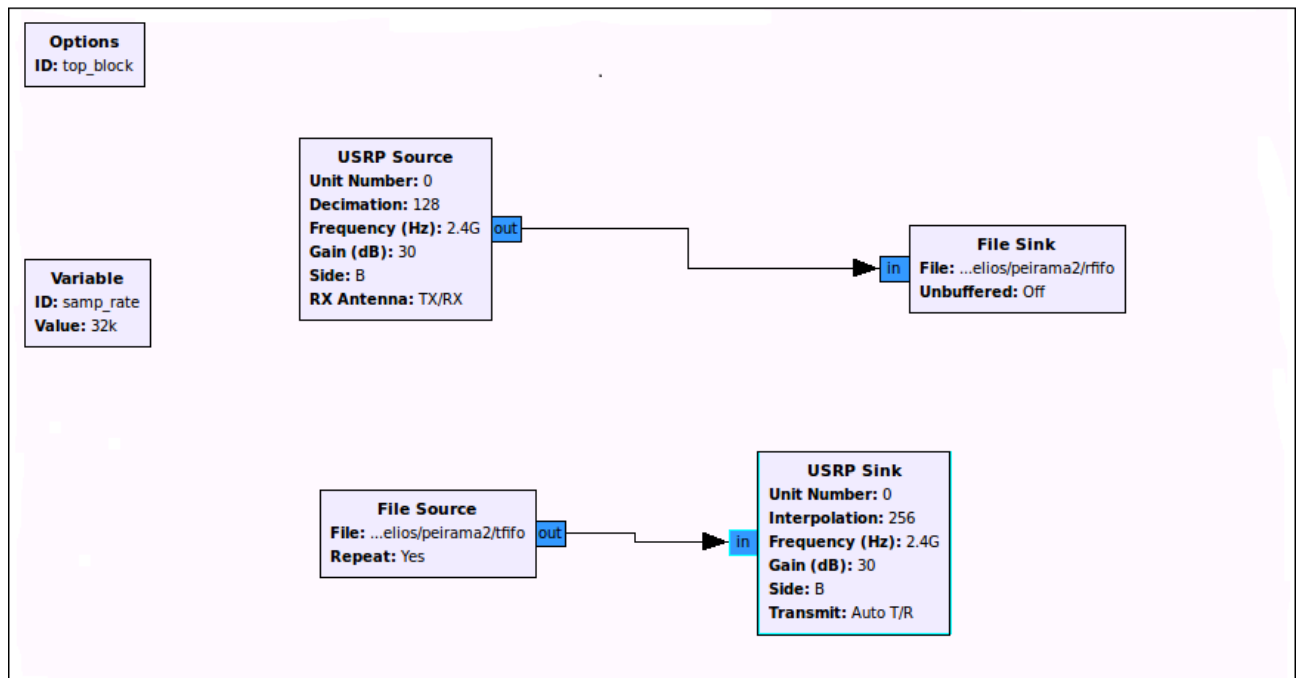


Figure 3.4: GNU Radio flowgraph for the single-antenna transceiver.

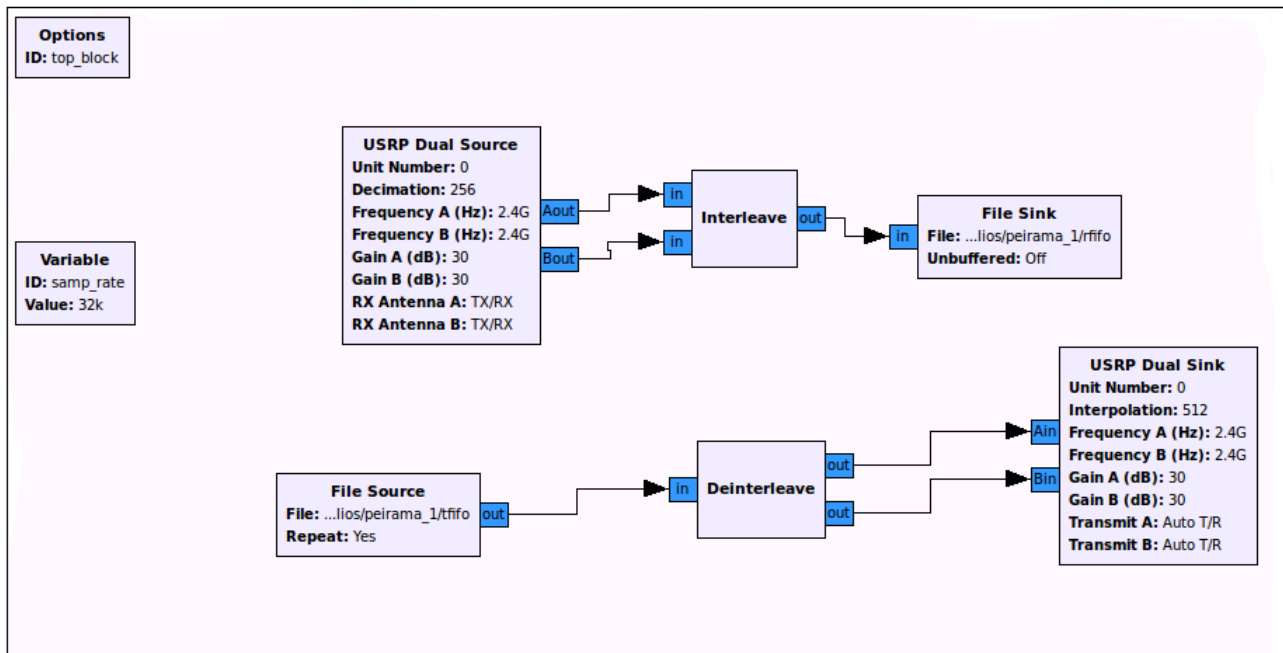


Figure 3.5: GNU Radio flowgraph for the two-antenna transceiver.

## 3.2 Processing methods

Here we discuss the basic DSP methods of our implementation. We consider packetized transmissions, with each packet consisting of  $L$  4-QAM symbols, pulse-shaped through SRRC filtering. All experiments take place in an indoor environment with close distance between the USRPs. The wireless channel can be well-modeled as flat-fading in frequency and block-fading in time, meaning that the channel coefficient remains constant for the duration of each packet.

### 3.2.1 Modulation

The ideal SRRC pulses are of infinite length. In practice we use truncated pulses, that are zero-valued outside the time interval  $[-AT, AT]$ , where  $T$  is the symbol-period. Therefore each pulse  $g(t)$  spans up to  $2A$  adjacent symbols. The corresponding discrete-time pulse can be

expressed as

$$g_n = \begin{cases} g(nT_s), & n \in [-AN, AN], \\ 0, & \text{otherwise,} \end{cases} \quad (3.1)$$

where  $T_s$  is the sample-period, and  $N = T/T_s$  expresses the oversampling factor. The scheduled for transmission symbol sequence  $X_l$ , is initially up-sampled by inserting  $N - 1$  zero-valued samples between the successive symbols. The produced up-sampled sequence  $\tilde{X}_k$  is then convolved with  $g_n$  to form the discrete-time signal

$$x_k = \sum_{n=-AN}^{AN} \tilde{X}_{k-n} g_n. \quad (3.2)$$

The corresponding continuous-time, transmitted baseband equivalent signal can be expressed as

$$x(t) = \sum_{l=0}^{L-1} X_l g(t - lT). \quad (3.3)$$

### 3.2.2 Synchronization and matched-filtering

A coarse synchronization with the transmitted symbols at each receive chain, is performed by measuring the energy ratio of two subsequent time windows, moving alongside the received samples. When this ratio becomes higher than a specified threshold, we assume that we have detected the beginning of a new packet. After the convolution with the matched filter  $\overleftarrow{g}_n = g_n$ , fine synchronization is achieved through exhaustive search over the detected packet, for the down-sampled by  $N$ ,  $L$ -sized sequence, with the highest energy.

### 3.2.3 Joint carrier-frequency-offset and channel estimation

The carrier frequency offset (CFO) impairment results in a remaining sinusoidal signal at the baseband output of each channel that rotates the received symbols and prevents coherent detection. Due to the phase coherence of the parallel transmit and receive chains in single-user MIMO systems, all paths suffer by a common CFO  $\Delta f$ . A  $(2 \times 2)$  signal model with the output

sampled at the symbol-time moments  $l = 0, 1, \dots, L - 1$ , can be expressed as

$$\begin{aligned} y_1[l] &= e^{j2\pi\nu l} \left( h_{11}x_1[l] + h_{12}x_2[l] \right) + w_1[l], \\ y_2[l] &= e^{j2\pi\nu l} \left( h_{21}x_1[l] + h_{22}x_2[l] \right) + w_2[l], \end{aligned} \tag{3.4}$$

where

- $y_j[l]$  is the received sample at receive antenna  $j$ , for  $j = 1, 2$ ,
- $x_i[l]$  is the transmitted symbol at each transmit antenna  $i$ , for  $i = 1, 2$ ,
- $h_{ij}$  is the baseband equivalent channel from the  $j$ -th transmit to the  $i$ -th receive antenna,
- $\nu = \Delta f \cdot T$  is the normalized cfo,
- $w_j[l]$  is the noise terms at each receive antenna, which can be well-modeled as i.i.d. circular white Gaussian.

Defining the vectors:

- $\mathbf{y}_1 = [y_1(0), \dots, y_1(L-1)]^T$ ,  $\mathbf{y}_2 = [y_2(0), \dots, y_2(L-1)]^T$  and  $\mathbf{y} = [\mathbf{y}_1^T, \mathbf{y}_2^T]^T$ ,
- $\mathbf{x}_1 = [x_1(0), x_1(1), \dots, x_1(L-1)]^T$  and  $\mathbf{x}_2 = [x_2(0), \dots, x_2(L-1)]^T$ ,
- $\mathbf{h} = [h_{11}, h_{12}, h_{21}, h_{22}]^T$ ,
- $\mathbf{w} = [w_1(0), \dots, w_1(L-1), w_2(0), \dots, w_2(L-1)]^T$ ,

and the matrices:

- $\mathbf{X} = \begin{pmatrix} \mathbf{x}_1 & \mathbf{x}_2 & \mathbf{0} & \mathbf{0} \\ \mathbf{0} & \mathbf{0} & \mathbf{x}_1 & \mathbf{x}_2 \end{pmatrix}$ , where  $\mathbf{0}$  denotes the  $L$ -dimensional zero-vector, and
- $\mathbf{\Gamma}(\nu) = \text{diag}([e^{j2\pi\nu 0}, \dots, e^{j2\pi\nu(L-1)}])$ ,

we can re-write (3.4) as

$$\mathbf{y} = \mathbf{\Gamma}(\nu)\mathbf{X}\mathbf{h} + \mathbf{w} \quad (3.5)$$

The ML-joint estimate of  $\nu$  maximizes the norm of the projection of  $\mathbf{\Gamma}^H(\nu)\mathbf{y}$  onto the column space of  $\mathbf{X}$ . It can be computed by exhaustive search over the set of the different possible values  $\tilde{\nu}$ , that is

$$\hat{\nu} = \arg \max_{\tilde{\nu} \in [-\frac{1}{2}, \frac{1}{2}]} \left( \|\mathbf{P}\mathbf{\Gamma}^H(\tilde{\nu})\mathbf{y}\| \right), \quad (3.6)$$

where  $\mathbf{P} = \mathbf{X}(\mathbf{X}^H\mathbf{X})^{-1}\mathbf{X}^H$ , is the projection matrix of  $\mathbf{X}$  [11].

After eliminating the CFO by applying the matrix  $\mathbf{\Gamma}^H(\hat{\nu})$  to  $\mathbf{y}$ , the corrected received symbol vector can be expressed by:

$$\hat{\mathbf{y}} = \mathbf{X}\mathbf{h} + \mathbf{w}. \quad (3.7)$$

The constellations before and after CFO elimination are depicted in Figure 3.6. After CFO correction, the ML-estimate  $\hat{\mathbf{h}}$  of the channel vector is computed by

$$\hat{\mathbf{h}} = (\mathbf{X}^H\mathbf{X})^{-1}\mathbf{X}^H\hat{\mathbf{y}}. \quad (3.8)$$

Due to the CFO impairment, the baseband channel estimate for multiple transmissions, suffers from arbitrary phase shifts even if the physical channel remains constant. Specifically, for the point to point case, the baseband channel estimations of two different transmissions  $k, k'$  during the coherence period of the physical channel, are related by:

$$h_k = e^{j\varphi}h_{k'}, \quad \varphi \sim \mathcal{U}[0, 2\pi) \quad (3.9)$$

where  $\varphi$  is the phase difference between the baseband channels  $h_k$  and  $h_{k'}$ , modeled as a uniform random variable. The four estimated channels in the  $(2 \times 2)$  case, for multiple transmissions under constant spatial conditions, are depicted in Figure (3.7).

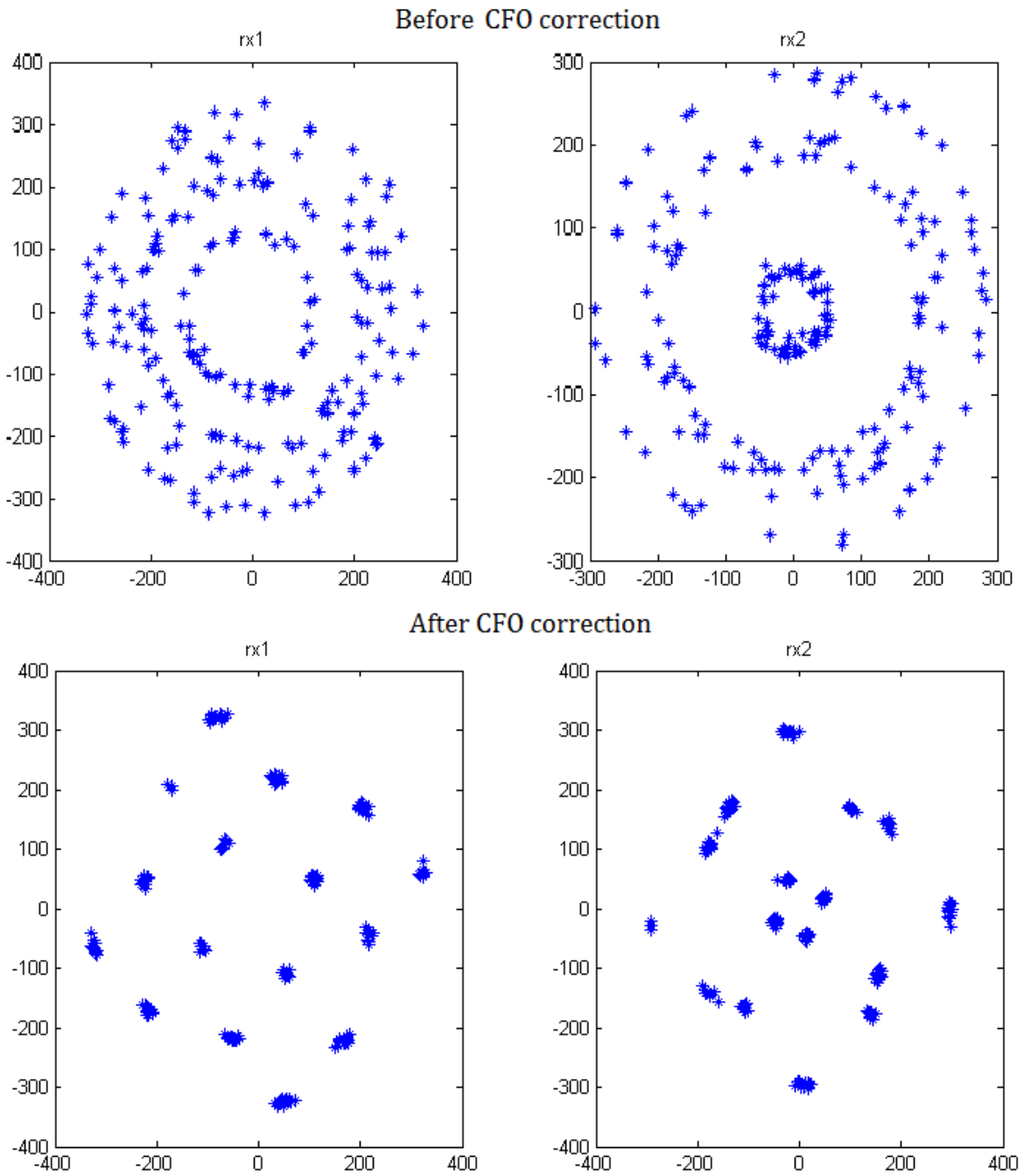


Figure 3.6: Received constellations before and after CFO correction.

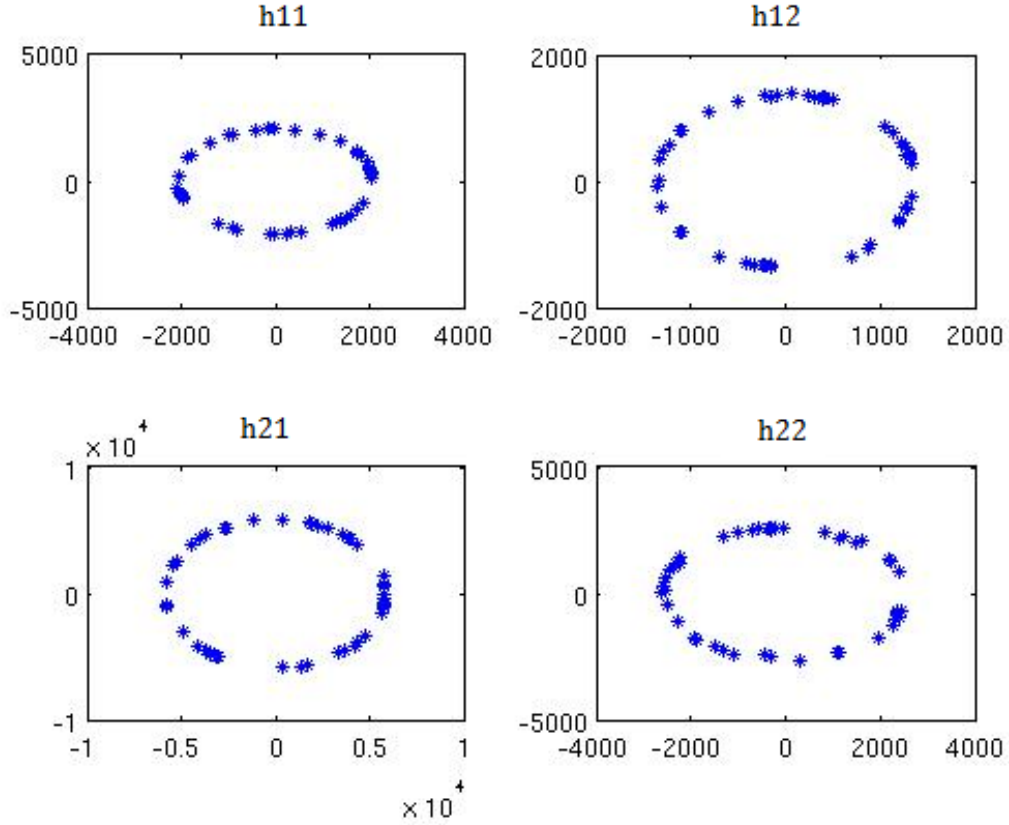


Figure 3.7: The estimated channels for multiple transmissions, under constant spatial conditions.

### 3.3 Single-user MIMO

We build a single-user  $(2 \times 2)$  MIMO system using two USRPs, each bearing two antennas for transmission and reception. Focusing on a certain time instant, the signal model can be expressed as

$$\mathbf{y} = \mathbf{H}\mathbf{x} + \mathbf{w}, \tag{3.10}$$

where

- $\mathbf{x} = [x_1, x_2]^T$  is the input vector, with elements the transmitted 4-QAM symbols from each transmit antenna,
- $\mathbf{y} = [y_1, y_2]^T$  is the output vector, with elements the received samples at each receive

antenna,

- $\mathbf{H} = \begin{pmatrix} h_{11} & h_{12} \\ h_{21} & h_{22} \end{pmatrix}$  is the corresponding channel matrix, and
- $\mathbf{w} = [w_1, w_2]^T$  is the noise vector.

### 3.3.1 Maximum-Likelihood detection

The maximum-likelihood estimate  $\hat{\mathbf{x}}_{ML}$ , of the transmitted vector  $\mathbf{x}$ , is computed through exhaustive search over the 2–dimensional set of the possible entries

$$\mathcal{X}^2 := \{[x_1, x_2]^T : (x_1, x_2) \in \mathcal{X} \times \mathcal{X}\}, \quad (3.11)$$

where  $\mathcal{X}$  is the 4-QAM constellation, and therefore  $|\mathcal{X}^2| = |\mathcal{X}|^2 = 16$ . After obtaining an estimate  $\tilde{\mathbf{H}}$  of the channel matrix, the receiver computes  $\hat{\mathbf{x}}_{ML}$  by

$$\hat{\mathbf{x}}_{ML} = \arg \min_{\hat{\mathbf{x}} \in \mathcal{X}^2} \left( \|\mathbf{y} - \tilde{\mathbf{H}}\hat{\mathbf{x}}\| \right). \quad (3.12)$$

### 3.3.2 Linear Zero-Forcing Equalization

For the equalization-based detection, the receiver applies the inverse  $\tilde{\mathbf{H}}^{-1}$  of the channel estimate on to  $\mathbf{y}$ , to obtain the equalized vector

$$\mathbf{y}_{ZF} = \mathbf{x} + \bar{\mathbf{w}}. \quad (3.13)$$

The received symbols before and after equalization are depicted in Figure 3.8.

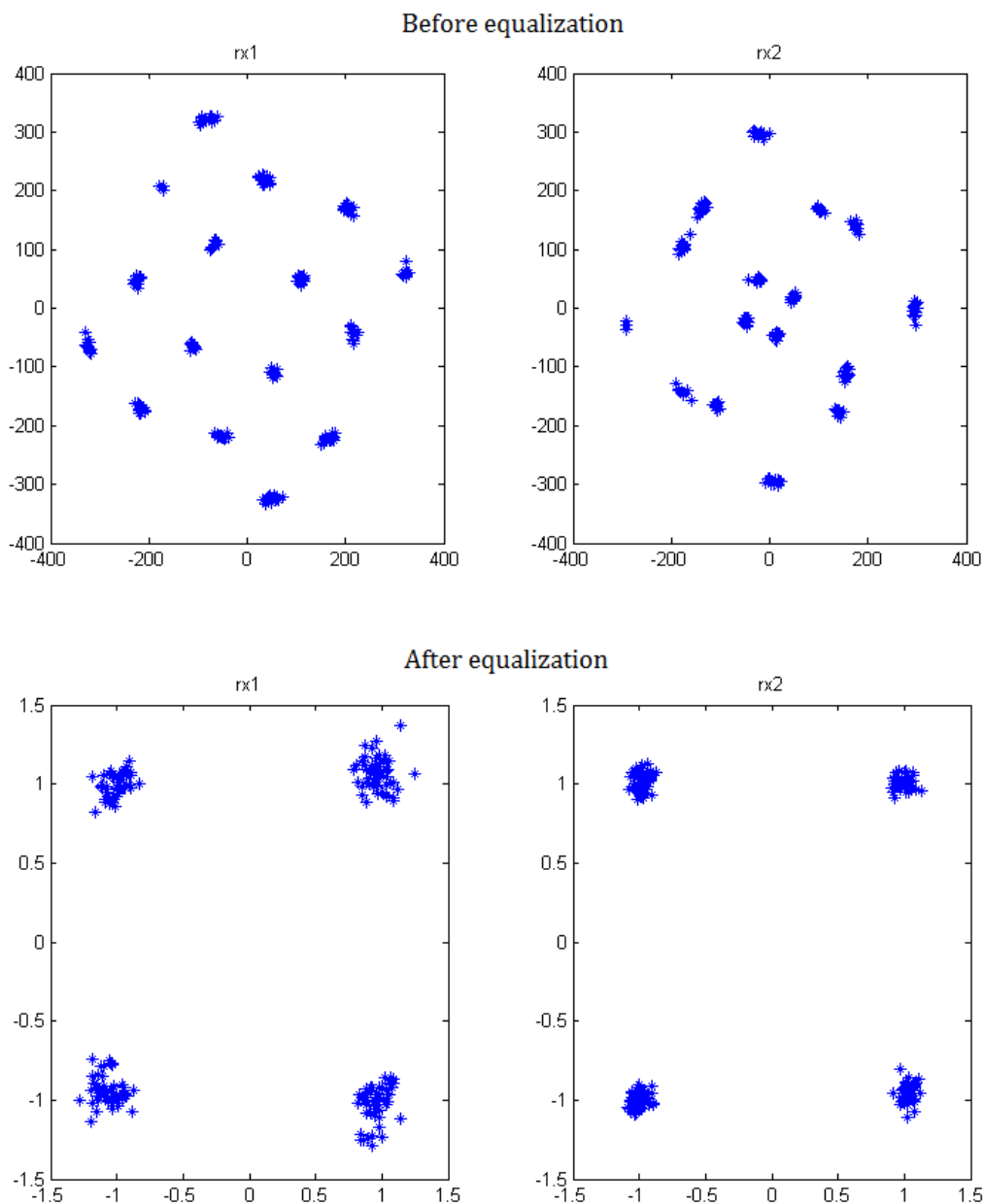


Figure 3.8: Received constellations before and after equalization.

### 3.3.3 Linear Zero-Forcing Pre-Equalization

We perform feedback based pre-equalization on the downlink channel. The process of linear pre-equalization can be described as follows:

- We initially transmit a packet of pilots symbols so that the receiver forms an estimate of the forward channel matrix.
- The channel estimate is further quantized and transformed into binary form. The produced bit sequence is subsequently mapped into data symbols that together with a number of pilot symbols form the feedback packet.
- The receiver feeds back the formed packet. The transmitter decodes the data-symbols and obtains the estimation of the forward channel  $\tilde{\mathbf{H}}$ . The transformed transmitted vector can be expressed as

$$\mathbf{x}_{ZF} = \beta \tilde{\mathbf{H}}^{-1} \mathbf{x} = \beta e^{-j2\pi\phi} \mathbf{H}^{-1} \mathbf{x}, \quad (3.14)$$

where  $\beta = \frac{\sqrt{2}}{\|\tilde{\mathbf{H}}^{-1}\|_F}$  is the normalization factor so that the total transmit power meets the initial power constraint.

Neglecting the estimation and quantization error, and assuming that the spatial conditions remain constant during the feedback process, the obtained matrix  $\tilde{\mathbf{H}}$  and the current channel matrix  $\mathbf{H}$  are related by

$$\tilde{\mathbf{H}} = e^{j2\pi\phi} \mathbf{H}, \quad (3.15)$$

where  $\phi$  is the random phase-offset common for all paths, due to the phase-coherence of the parallel transmit and receive chains. The receiver gets

$$\mathbf{y}_{ZF} = \mathbf{H} \mathbf{x}_{ZF} + \mathbf{w} = \mathbf{H} (\beta e^{-j2\pi\phi} \mathbf{H}^{-1} \mathbf{x}) + \mathbf{w} = \beta e^{-j2\pi\phi} \mathbf{x} + \mathbf{w}. \quad (3.16)$$

The received constellations are depicted in Figure (3.9), where we can notice the effect of the phase-offset  $e^{-j2\pi\phi}$ . The term  $\beta e^{-j2\pi\phi}$  is estimated through pilot symbols at the receiver. After the estimation, the decision over the transmitted vector  $\mathbf{x}$  is taken based on the transformed vector

$$\bar{\mathbf{y}}_{ZF} = (\beta e^{-j2\pi\phi})^{-1} \mathbf{y}_{ZF} = \mathbf{x} + \underbrace{\beta^{-1} e^{j2\pi\phi} \mathbf{w}}_{\bar{\mathbf{w}}} = \mathbf{x} + \bar{\mathbf{w}}. \quad (3.17)$$

In Figure (3.10), we see the constellations of a series of packets, pre-equalized based on the same channel estimate, transmitted over a dynamically changing channel. As we can see the outdated CSI reintroduces co-channel interference and the receiver gradually gets linear combinations of the parallel transmitted symbols.

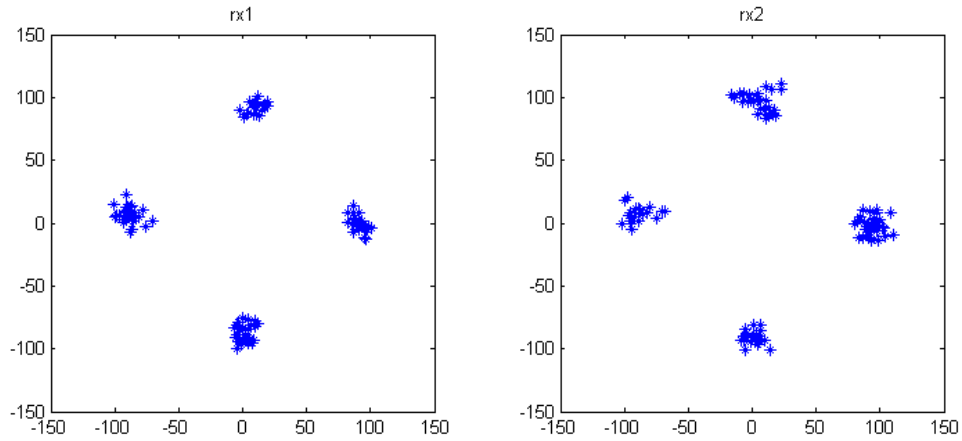


Figure 3.9: Pre-equalized received constellation.

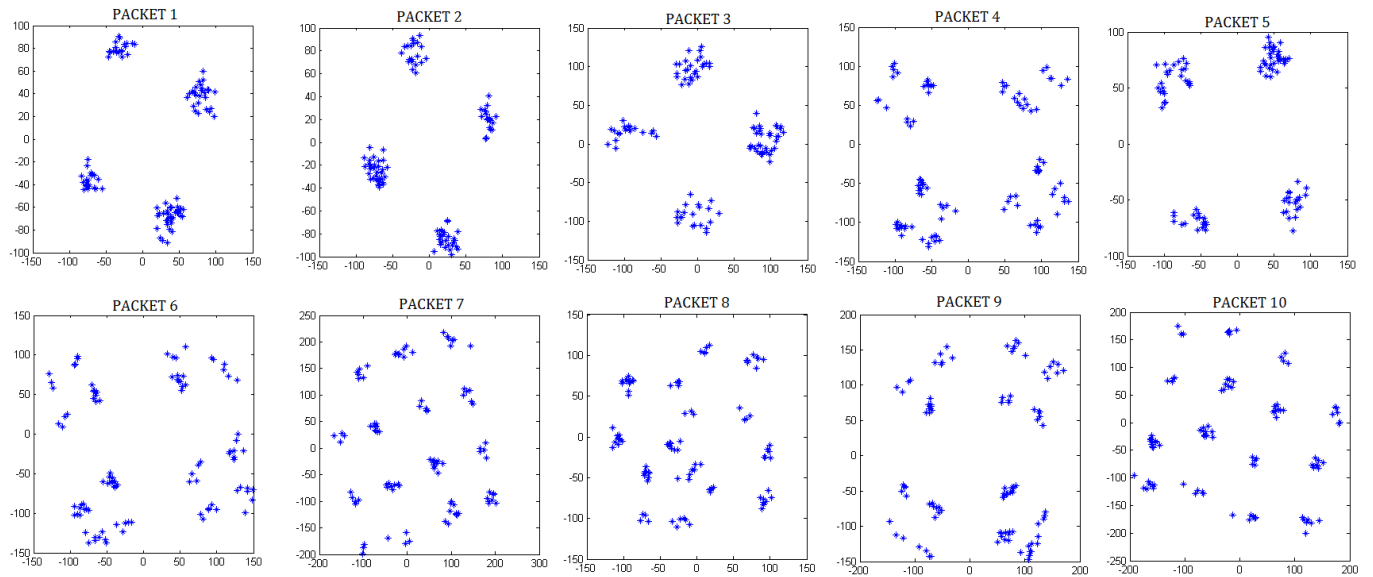


Figure 3.10: Received pre-equalized constellations for multiple transmitted packets, over dynamic channel.

### 3.3.4 Performance

#### Evaluation method

In order to evaluate the performance of equalization and pre-equalization with respect to the optimal ML-detection rule, one USRP acts as the BS and the other to act as the USER which performs BER measurements over the transmitted symbols.

- At the first stage, the BS transmits a series of subsequent packets at the downlink. The USER performs ML-detection and equalization at the received packets and measures the bit errors for each detection method.
- At the second stage, the USER feeds back the estimated downlink channel to the BS and waits for the pre-equalized packets.
- Finally, the BS decodes the feedback packet and transmits a series of pre-equalized symbols, through which the USER measures the bit errors for the pre-equalization method.

The above process is repeated for various different transmit gain values, in order to obtain BERs for varied received SNR.

#### The transmitted packet

The structure of the packet based on which we perform the BER measurements, is depicted in Figure (3.11). It is divided into the following parts:

- Head: The head of the packet consists of a number of pilot symbols transmitted in high SNR, that are exploited by the USER for synchronization and CFO estimation.
- Main packet: The main packet consists of symbols in varying SNR, based on which the USER performs the BER measurements. 25% of this part consists of pilot symbols that are used for estimating the downlink channel.

- Tail: The tail consists of a small number of pilot symbols in high SNR, to ensure that the USER receives the whole transmitted packet.

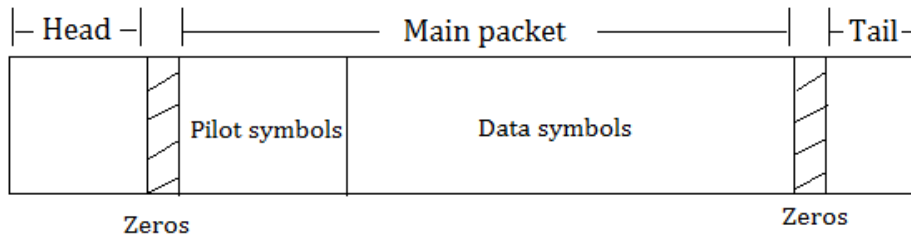


Figure 3.11: The transmitted packet for the BER measurements.

## Results

The resulting BERs subject to various received SNRs, are depicted in Figure (3.12).

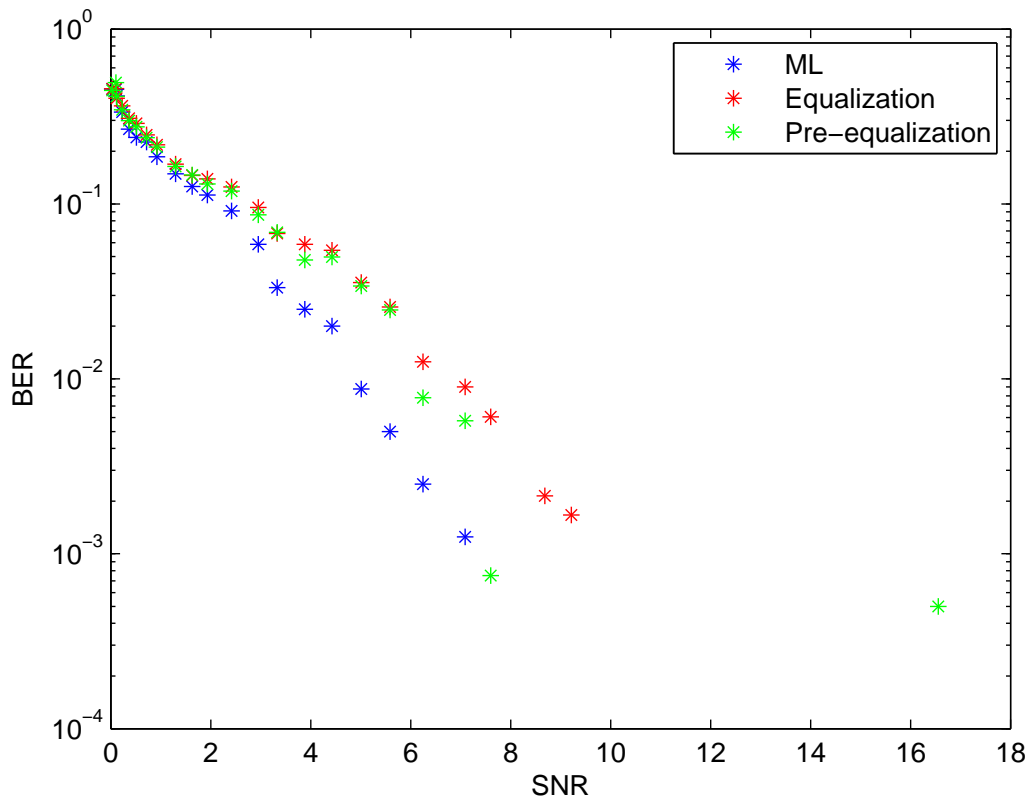


Figure 3.12: BER results.

## 3.4 Multi-user MIMO

We build a multi-user ( $2 \times 2$ ) system using one USRP with two antennas, denoted as the BS, and two single-antenna USRPs, denoted as the USERS.

### 3.4.1 Feedback based Pre-equalization

The process of downlink pre-equalization through feedback from the two users can be described as follows:

- The BS initially sends pilot packets to the downlink. User A sends its feedback packet first while USER B is listening.
- Then user B detects the end of transmission of the first user and starts its own feedback transmission.
- The BS decodes the two packets to obtain the downlink channel estimation, and transmits a series of pre-equalized packets to the users.

Neglecting the estimation and quantization error, and assuming that the spatial conditions remain constant during the feedback process, the obtained downlink matrix  $\tilde{\mathbf{H}}$  and the current downlink channel matrix  $\mathbf{H}$  are related by

$$\tilde{\mathbf{H}} = \begin{pmatrix} e^{j2\pi\phi_1} h_{11} & e^{j2\pi\phi_1} h_{12} \\ e^{j2\pi\phi_2} h_{21} & e^{j2\pi\phi_2} h_{22} \end{pmatrix} \quad (3.18)$$

(3.19)

$$= \underbrace{\begin{pmatrix} e^{j2\pi\phi_1} & 0 \\ 0 & e^{j2\pi\phi_2} \end{pmatrix}}_{\mathbf{D}} \begin{pmatrix} h_{11} & h_{12} \\ h_{21} & h_{22} \end{pmatrix} \quad (3.20)$$

(3.21)

$$= \mathbf{D} \cdot \mathbf{H}. \quad (3.22)$$

The transmitted pre-equalized symbol vector can be expressed as

$$\mathbf{x}_{ZF} = \beta \tilde{\mathbf{H}}^{-1} \mathbf{x} = \beta \mathbf{H}^{-1} \mathbf{D}^{-1} \mathbf{x} = \beta \mathbf{H}^{-1} \mathbf{D}^* \mathbf{x}, \quad (3.23)$$

where  $\mathbf{D}^* = \text{diag}([e^{-j2\pi\phi_1}, e^{-j2\pi\phi_2}])$ . The received vector (Fig. 3.13) is given by

$$\mathbf{y}_{ZF} = \begin{bmatrix} y_{ZF,1} \\ y_{ZF,2} \end{bmatrix} = \mathbf{H} \mathbf{x}_{ZF} + \mathbf{w} = \mathbf{H} (\beta \mathbf{H}^{-1} \mathbf{D}^* \mathbf{x}) + \mathbf{w} = \beta \mathbf{D}^* \mathbf{x} + \mathbf{w}. \quad (3.24)$$

Each user  $i$ , for  $i = 1, 2$ , receives  $y_{ZF,i} = \beta e^{-j2\pi\phi_i} x_i$ , estimates the phase and amplitude shift through pilot symbols and performs equalization.

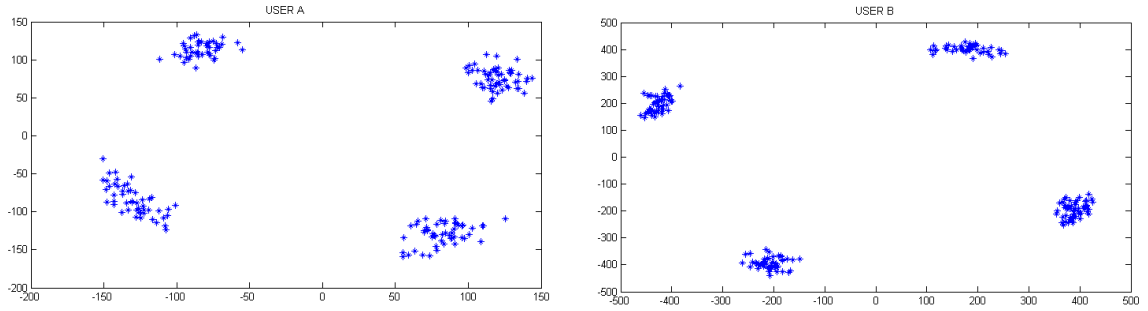


Figure 3.13: Received pre-equalized constellations for the two Users.

### 3.4.2 Exploiting the up-link CSI

#### Effect of non-reciprocal transceivers in reverse-channel estimation

Since different circuitry is used for the transmission and the reception of signals (high power/low noise amplifiers, DAC/ADC etc), the transmit and receive chains of a typical transceiver are generally not reciprocal. A model for the effective downlink and uplink channel paths in a ( $2 \times 2$ ) system, is depicted in Figure (3.14). Assuming that the mutual coupling and reflections

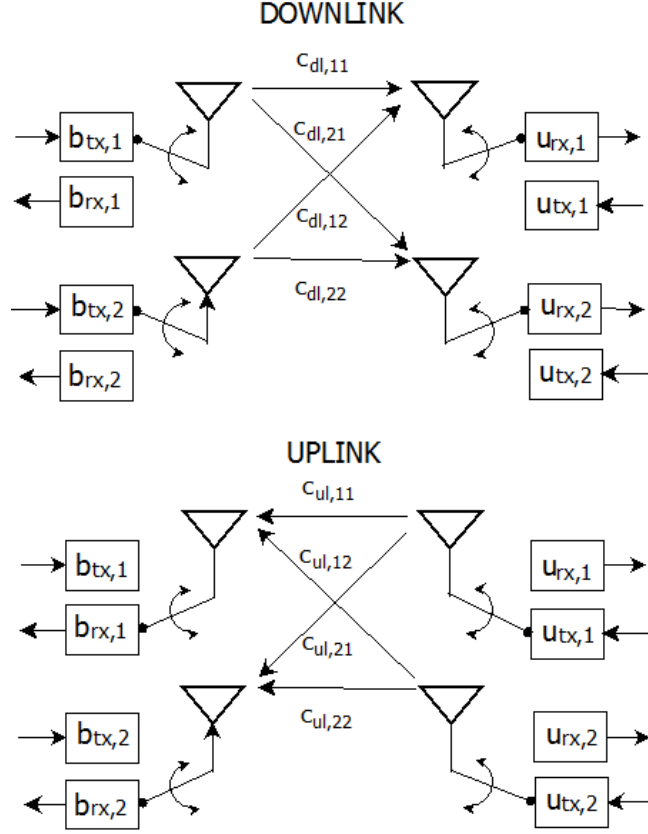


Figure 3.14: Pre-equalized constellations for the two users.

parameters are negligible, the effective downlink channel can be analyzed to [12]:

$$\begin{aligned}
 \mathbf{H}_{dl} &= \begin{pmatrix} h_{dl,11} & h_{dl,21} \\ h_{dl,12} & h_{dl,22} \end{pmatrix} = \begin{pmatrix} b_{tx,1} & c_{dl,11} & u_{rx,1} & b_{tx,2} & c_{dl,21} & u_{rx,1} \\ b_{tx,1} & c_{dl,12} & u_{rx,2} & b_{tx,2} & c_{dl,22} & u_{rx,2} \end{pmatrix} \\
 &= \begin{pmatrix} u_{rx,1} & 0 \\ 0 & u_{rx,2} \end{pmatrix} \begin{pmatrix} c_{dl,11} & c_{dl,21} \\ c_{dl,12} & c_{dl,22} \end{pmatrix} \begin{pmatrix} b_{tx,1} & 0 \\ 0 & b_{tx,2} \end{pmatrix} \\
 &= \mathbf{U}_{rx} \cdot \mathbf{C}_{dl} \cdot \mathbf{B}_{tx}, \tag{3.25}
 \end{aligned}$$

where

- the terms  $h_{dl,ij}$  express the effective down-link channel paths between the  $i$ th transmit

and the  $j$ th receive chain,

- the terms  $c_{dl,ij}$  the corresponding reciprocal physical paths,
- the terms  $b_{tx,i}$  and  $b_{rx,i}$  the factors induced by each transmit and receive chain of the basestation respectively and
- the terms  $u_{tx,i}$  and  $u_{rx,i}$  the corresponding factors induced by the transmit and receive chains of the user

In the same manner the effective uplink channel can be analyzed to:

$$\begin{aligned}
\mathbf{H}_{ul}^T &= \begin{pmatrix} h_{ul,11} & h_{ul,21} \\ h_{ul,12} & h_{ul,22} \end{pmatrix} = \begin{pmatrix} b_{rx,1} c_{ul,11} u_{tx,1} & b_{rx,2} c_{ul,12} u_{tx,1} \\ b_{rx,1} c_{ul,21} u_{tx,2} & b_{rx,2} c_{ul,22} u_{tx,2} \end{pmatrix} \\
&= \begin{pmatrix} u_{tx,1} & 0 \\ 0 & u_{tx,2} \end{pmatrix} \begin{pmatrix} c_{ul,11} & c_{ul,12} \\ c_{ul,21} & c_{ul,22} \end{pmatrix} \begin{pmatrix} b_{rx,1} & 0 \\ 0 & b_{rx,2} \end{pmatrix} \\
&= \mathbf{U}_{tx} \cdot \mathbf{C}_{ul}^T \cdot \mathbf{B}_{rx}
\end{aligned} \tag{3.26}$$

Since the physical channel is reciprocal, it holds that

$$\mathbf{C}_{dl} = \mathbf{C}_{ul}^T. \tag{3.27}$$

By (3.25),(3.27) and (3.26) we get that

$$\mathbf{H}_{ul}^T = \underbrace{\mathbf{U}_{tx} \mathbf{U}_{rx}^{-1}}_{\mathbf{U}_{[tx/rx]}} \mathbf{H}_{dl} \underbrace{\mathbf{B}_{tx}^{-1} \mathbf{B}_{rx}}_{\mathbf{B}_{[rx/tx]}} \tag{3.28}$$

$$= \mathbf{U}_{[tx/rx]} \mathbf{H}_{dl} \mathbf{B}_{[rx/tx]}. \tag{3.29}$$

For ideal reciprocal transceivers the diagonal matrices  $B_{[rx/tx]}$  and  $U_{[tx/rx]}$  are equal with the identity matrix  $\mathbf{I}$ . In practice, the gains of the transmit and receive chain are generally unequal and therefore  $\mathbf{B}_{[rx/tx]}, \mathbf{U}_{[tx/rx]} \neq \mathbf{I}$ . In that case, pre-equalizing directly based on  $\mathbf{H}_{ul}^T$  results in

$$\mathbf{y}_{ZF} = \mathbf{H}_{dl} \mathbf{H}_{ul}^{-T} \mathbf{x} + \mathbf{w} \quad (3.30)$$

$$= \mathbf{H}_{dl} \mathbf{B}_{[rx/tx]}^{-1} \mathbf{H}_{dl}^{-1} \mathbf{U}_{[tx/rx]}^{-1} \mathbf{x} + \mathbf{w} \quad (3.31)$$

If the diagonal elements of  $\mathbf{B}_{[rx/tx]}$  are unequal that is if

$$\frac{b_{rx,1}}{b_{tx,1}} \neq \frac{b_{rx,2}}{b_{tx,2}} \Leftrightarrow \frac{b_{rx,1} b_{tx,2}}{b_{tx,1} b_{rx,2}} \neq 1, \quad (3.32)$$

which is usually the case, the product  $(\mathbf{H}_{dl} \mathbf{B}_{[rx/tx]}^{-1} \mathbf{H}_{dl}^{-1})$  results in a non-diagonal matrix, and prevents interference-cancellation. Therefore,  $\mathbf{H}_{ul}^{-T}$  cannot be used directly for pre-equalizing over the downlink channel.

### Calibration method

The calibration method proposed in [12], utilizes the Total Least-Squares method to compensate for the error induced by the matrices  $\mathbf{B}_{[rx/tx]}$  and  $\mathbf{U}_{[tx/rx]}$  in the uplink estimation. We implement a simpler approach in which we estimate and normalize the term  $cal = \frac{b_{rx,1} b_{tx,2}}{b_{tx,1} b_{rx,2}}$  in (3.32). Utilizing the estimates of the uplink and downlink paths between the BS and the first user, we compute the above term by calculating the ratio

$$\frac{h_{ul,11} h_{dl,11}^{-1}}{h_{ul,21} h_{dl,12}^{-1}} = \frac{b_{rx,1} c_{ul,11} u_{tx,1} (u_{rx,1} c_{dl,11} b_{tx,1})^{-1}}{b_{rx,2} c_{ul,21} u_{tx,1} (u_{rx,1} c_{dl,12} b_{tx,2})^{-1}} = \frac{b_{rx,1} b_{tx,2}}{b_{tx,1} b_{rx,2}} = cal. \quad (3.33)$$

The same result can be extracted by using the second user as reference, by calculating the ratio  $\frac{h_{ul,12} h_{dl,21}^{-1}}{h_{ul,22} h_{dl,22}^{-1}}$ . Measurements of the calibration term  $cal$  based on both USRP Users, are depicted

in Figure (3.15). After estimating  $cal$ , the uplink estimate  $\mathbf{H}_{ul}^T$  can be transformed as in:

$$\tilde{\mathbf{H}}_{ul}^T = \mathbf{H}_{ul}^T \text{diag}([1, cal]) = \mathbf{U}_{[tx/rx]} \mathbf{H}_{dl} \mathbf{B}_{[rx/tx]} \text{diag}([1, cal]).$$

where

$$\begin{aligned} \mathbf{B}_{[rx/tx]} \text{diag}([1, cal]) &= \text{diag} \left( \begin{bmatrix} \frac{b_{rx,1}}{b_{tx,1}} & \frac{b_{rx,2}}{b_{tx,2}} \end{bmatrix} \right) \text{diag} \left( \begin{bmatrix} 1 & \frac{b_{rx,1} b_{tx,2}}{b_{tx,1} b_{rx,2}} \end{bmatrix} \right) \\ &= \text{diag} \left( \begin{bmatrix} \frac{b_{rx,1}}{b_{tx,1}} & \frac{b_{rx,1}}{b_{tx,1}} \end{bmatrix} \right), \end{aligned} \quad (3.34)$$

therefore

$$\begin{aligned} \tilde{\mathbf{H}}_{ul}^T &= \mathbf{U}_{[tx/rx]} \mathbf{H}_{dl} \text{diag} \left( \begin{bmatrix} \frac{b_{rx,1}}{b_{tx,1}} & \frac{b_{rx,1}}{b_{tx,1}} \end{bmatrix} \right) \\ &= \frac{b_{rx,1}}{b_{tx,1}} \mathbf{U}_{[tx/rx]} \mathbf{H}_{dl}. \end{aligned} \quad (3.35)$$

By (3.35), we can see that each row vector of the transformed estimate  $\tilde{\mathbf{H}}_{ul}^T$  is parallel with the corresponding row vector of the downlink estimate  $\mathbf{H}_{dl}$ . Thus  $\tilde{\mathbf{H}}_{ul}^T$  is suitable for pre-canceling interference over the row space of  $\mathbf{H}_{dl}$ .

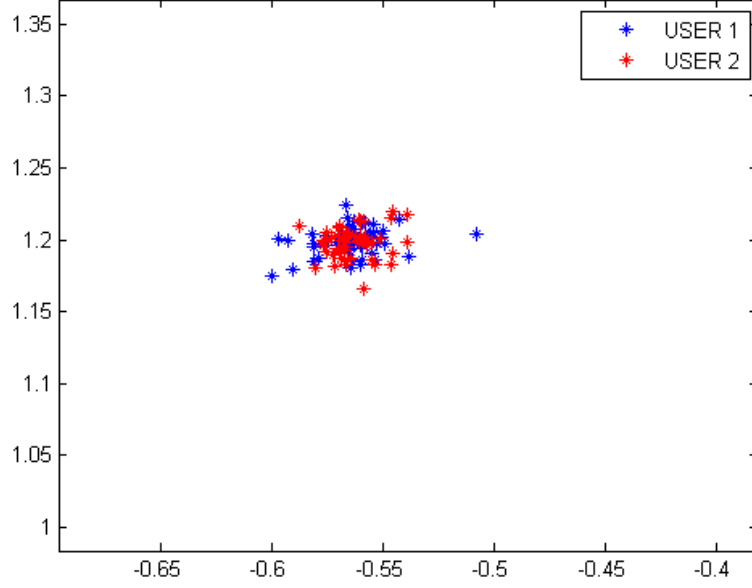


Figure 3.15: The term  $cal = \frac{b_{rx,1}b_{tx,2}}{b_{tx,1}b_{rx,2}}$  estimated using each of the two users as reference.

### Pre-equalizing based on reverse-link channel estimation

The process of exploiting the uplink estimation to perform Pre-equalization for the downlink channel can be summarized into the following steps:

- At the first stage, the BS starts the calibration procedure, by sending training packets on the downlink channel. One of the two users feeds back its downlink estimate, along with training symbols. Through the feed-back packet, the BS obtains the required downlink and uplink channel estimate and computes the calibration factor  $cal$ .
- After the calibration phase, we dynamically change the channel and the two users successively send their training packets at the uplink.
- The BS obtains the updated uplink CSI and calculates the transformed estimation  $\tilde{\mathbf{H}}_{ul}^T = \mathbf{H}_{ul}^T \text{diag}([1, cal])$ . The transmitted pre-equalized symbol vector can be expressed as

$$\mathbf{x}_{ZF} = \beta \tilde{\mathbf{H}}_{ul}^{-T} \mathbf{x}, \quad (3.36)$$

where  $\beta = \frac{\sqrt{2}}{\|\tilde{\mathbf{H}}_{ul}^{-T}\|_F}$  is the normalization factor.

Taking into account the random phase-offsets and assuming perfect CSI,  $\tilde{\mathbf{H}}_{ul}^T$  and the actual downlink channel matrix  $\mathbf{H}_{dl}$  are related by

$$\tilde{\mathbf{H}}_{ul}^T = \frac{b_{rx,1}}{b_{tx,1}} \mathbf{D} \mathbf{U}_{[tx/rx]} \mathbf{H}_{dl}, \quad (3.37)$$

where  $\mathbf{D} = \text{diag}([e^{j2\pi\phi_1}, e^{j2\pi\phi_2}])$ . The received vector (Figure 3.16) is given by

$$\begin{aligned} \mathbf{y}_{ZF} &= \begin{bmatrix} y_{ZF,1} \\ y_{ZF,2} \end{bmatrix} = \mathbf{H}_{dl} \mathbf{x}_{ZF} + \mathbf{w} \\ &= \mathbf{H}_{dl} \beta \tilde{\mathbf{H}}_{ul}^{-T} \mathbf{x} + \mathbf{w} \\ &= \mathbf{H}_{dl} \beta \left( \frac{b_{rx,1}}{b_{tx,1}} \right)^{-1} \mathbf{H}_{dl}^{-1} \mathbf{U}_{[tx/rx]}^{-1} \mathbf{D}^{-1} \mathbf{x} + \mathbf{w} \\ &= \beta \frac{b_{tx,1}}{b_{rx,1}} \mathbf{U}_{[rx/tx]} \mathbf{D}^* \mathbf{x} + \mathbf{w}. \end{aligned} \quad (3.38)$$

Each user  $i$ , for  $i = 1, 2$ , estimates the phase and amplitude shift through pilot symbols and performs equalization.

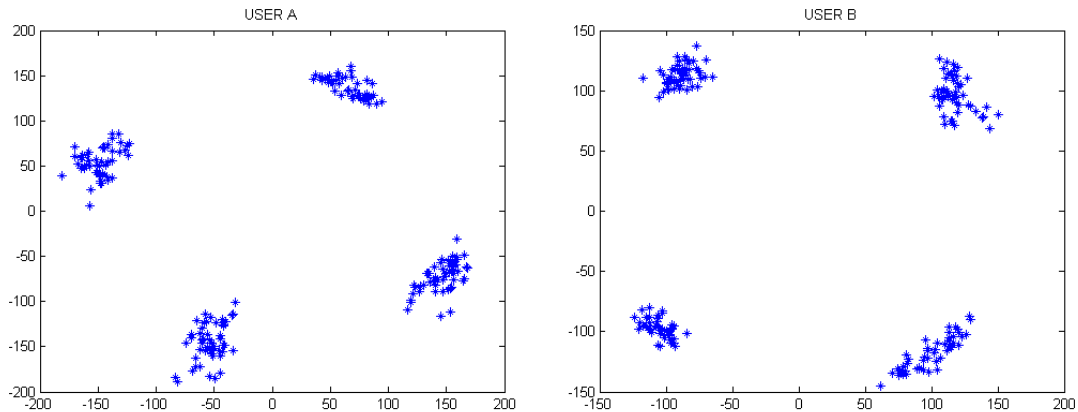


Figure 3.16: Received pre-equalized constellations, based on uplink CSI.

# Chapter 4

## Conclusions and future work

We described and implemented linear equalization in a 2-input/2-output single-user system, as well as linear pre-equalization through feedback from the receiver, under static channel conditions. We also implemented feedback-based linear pre-equalization in a 2-user system with a 2-antenna BS and single-antenna users, in spite of the different phase-shifts that each user experiences. The above result is a logical consequence of the fact that interference cancellation is performed at the level of the antennas, and is not affected by the random phase induced during down-conversion of the signal from RF to baseband. Finally in the 2-user case, we successfully performed pre-equalization based on reverse-channel estimation, in spite of the non-reciprocal transmit and receive chains of the USRPs, through a software-based calibration procedure. The calibration parameters remain (approximately) constant after the initialization of the USRPs, and therefore the calibration needed only to be performed once, at the beginning of the experiment.

As a future work, it can be suggested the implementation of the above techniques for Orthogonal Frequency Division Multiplexing (OFDM) systems.

# Bibliography

- [1] Athanasios Liavas, “Telecommunication Systems,” *course notes*.
- [2] Amos Lapidoth, “A Foundation in Digital Communication,” *Cambridge University Press*, 2009.
- [3] Athanasios Liavas, “Wireless Communication,” *course notes*.
- [4] David Tse and Pramod Viswanath, “Fundamentals of Wireless Communication,” *Cambridge University Press*, 2005.
- [5] Dominik Seethaler, Harold Artes, and Franz Hlawatsch, “Detection Techniques for MIMO Spatial Multiplexing Systems,” *Elektrotechnik und Informationstechnik*, March 2005.
- [6] Christoph Windpassinger, Robert F.H. Fischer, Tomas Vencel, Johannes B. Huber, “Pre-coding in Multi-Antenna and Multi-User Communications,” *IEEE Transactions on Wireless Communications*, July 2004.
- [7] H. Lütkepohl, “Handbook of Matrices,” *Wiley*, 1996, page 43.
- [8] SDR Forum, “SDRF Cognitive Radio Definitions ,” *Working Document SDRF*,  
URL: [http://www.sdrforum.org/pages/documentLibrary/documents/SDRF-06-R-0011-V1\\_0\\_0.pdf](http://www.sdrforum.org/pages/documentLibrary/documents/SDRF-06-R-0011-V1_0_0.pdf).
- [9] GNU Radio Wiki, URL: <http://gnuradio.org/redmine/projects/gnuradio/wiki>.
- [10] Ettus Knowledge Base, URL: <http://www.ettus.com/kb/>.

- [11] Michele Morelli and Umberto Mengali, “Carrier-frequency estimation for transmissions over selective channels,” *IEEE Transactions on Communications*, vol. 48, no. 9, September 2000.
- [12] Mark Petermann, Dirk Wubben, and Karl-Dirk Kammeyer, “Calibration of Non-Reciprocal Transceivers for Linearly Pre-Equalized MU-MISO-OFDM Systems in TDD Mode,” *Department of Communications Engineering University of Bremen*, Bremen, Germany.